Hemilabile Proton Relays and Redox-Activity Lead to {FeNO}^{x} and Significant Rate Enhancements in NO_2^- Reduction.

Pui Man Cheung,[†] Kyle T. Burns,[†] Yubin M. Kwon,[†] Megan Y. Deshaye,[†] Kristopher J. Aguayo[†] Victoria F. Oswald,[§] Takele Seda,[⊥] Lev N. Zakharov,[‡] Tim Kowalczyk,[*†] and John D. Gilbertson[*,†]

[†]Department of Chemistry and [⊥]Physics, Western Washington University, Bellingham, Washington 98225, United States

[‡]Department of Chemistry, University of Oregon, Eugene, Oregon 97403, United States

[§]Department of Chemistry, University of California, Irvine, Irvine, California 92697, United States

Corresponding Authors

*Email: john.gilbertson@wwu.edu, tim.kowalczyk@wwu.edu

Table of Contents **Page**

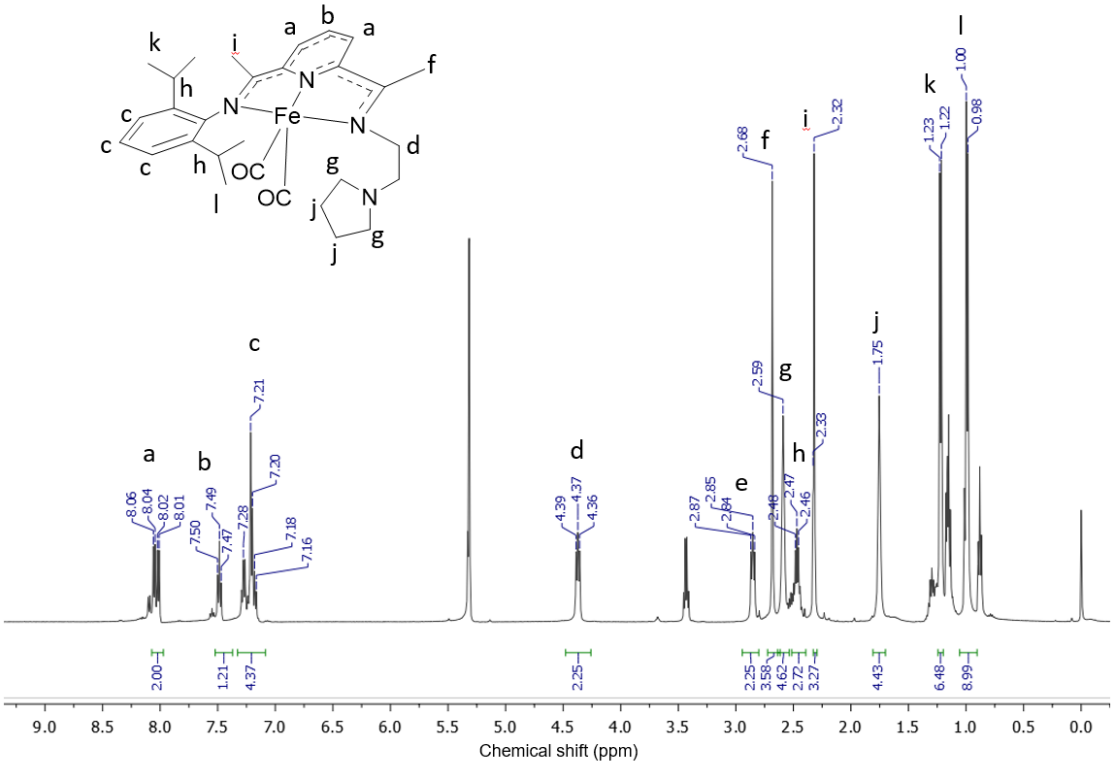

Figure S1. ^{1}H NMR of Fe(^{Pyrr}PDI)(CO)$_2$ (**3**), 500 MHz, CD_2Cl_2.

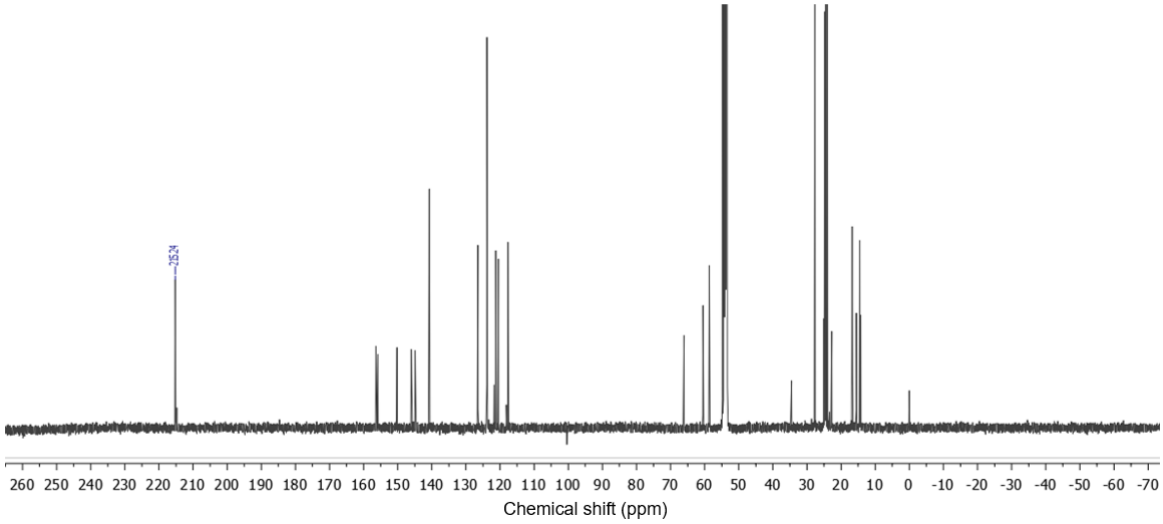

Figure S2. ^{13}C{^{1}H} NMR of Fe(^{Pyrr}PDI)(CO)$_2$ (**3**), 500 MHz, CD_2Cl_2.

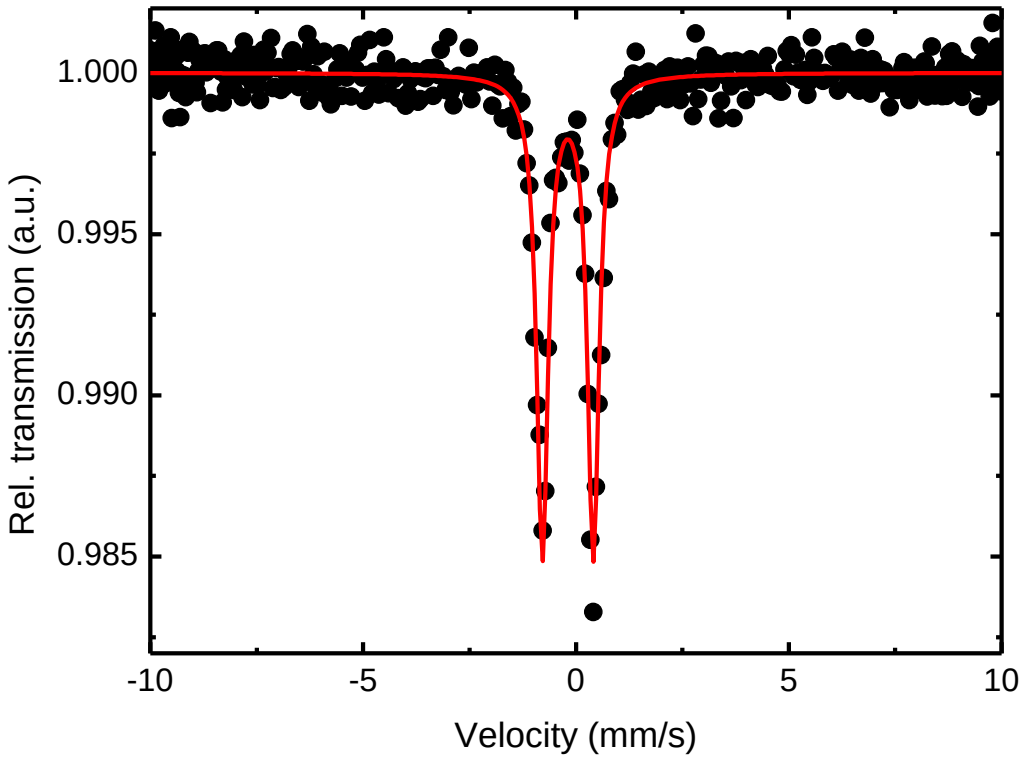

Figure S3. Room temperature zero-field Mössbauer spectrum of Fe(^{Pyrr}PDI)(CO)$_2$ (**3**); δ = -0.089(3) mm/s, ΔE_Q = 1.197(3) mm/s, Line width, Γ = 0.326(7) mm/s.

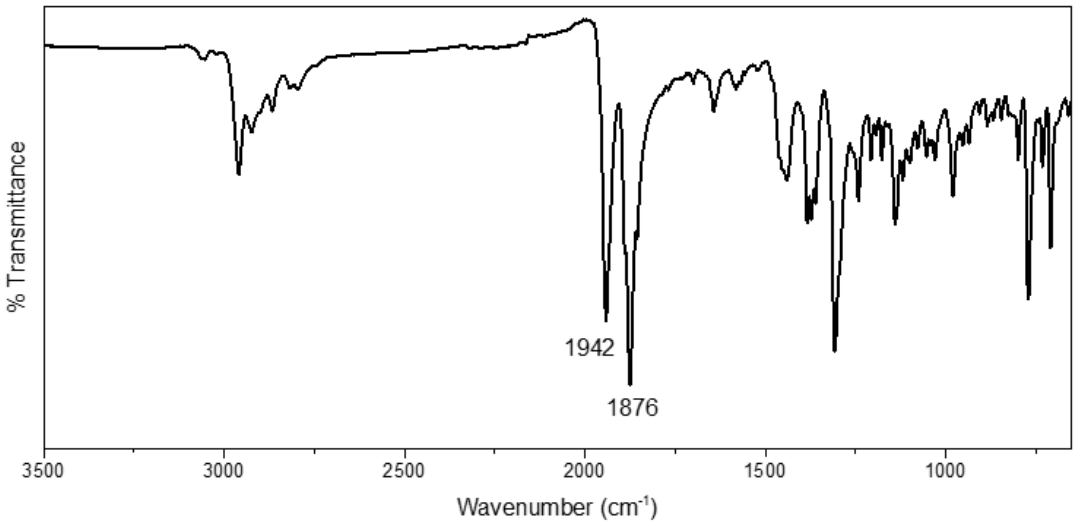

Figure S4. Solid FT-IR ATR spectrum of Fe(^{Pyrr}PDI)(CO)$_2$ (**3**).

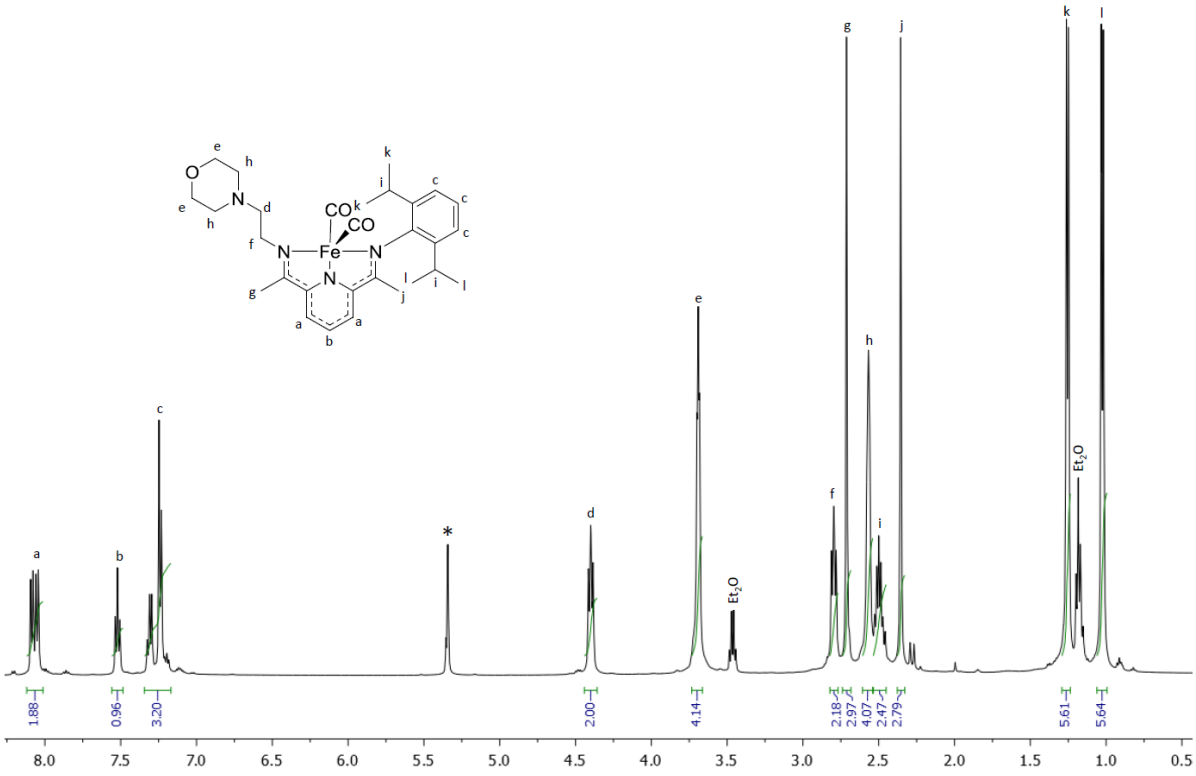

Figure S5. ^{1}H NMR of Fe(^{Mor}PDI)(CO)$_2$ (**4**), 500 MHz, CD_2Cl_2.

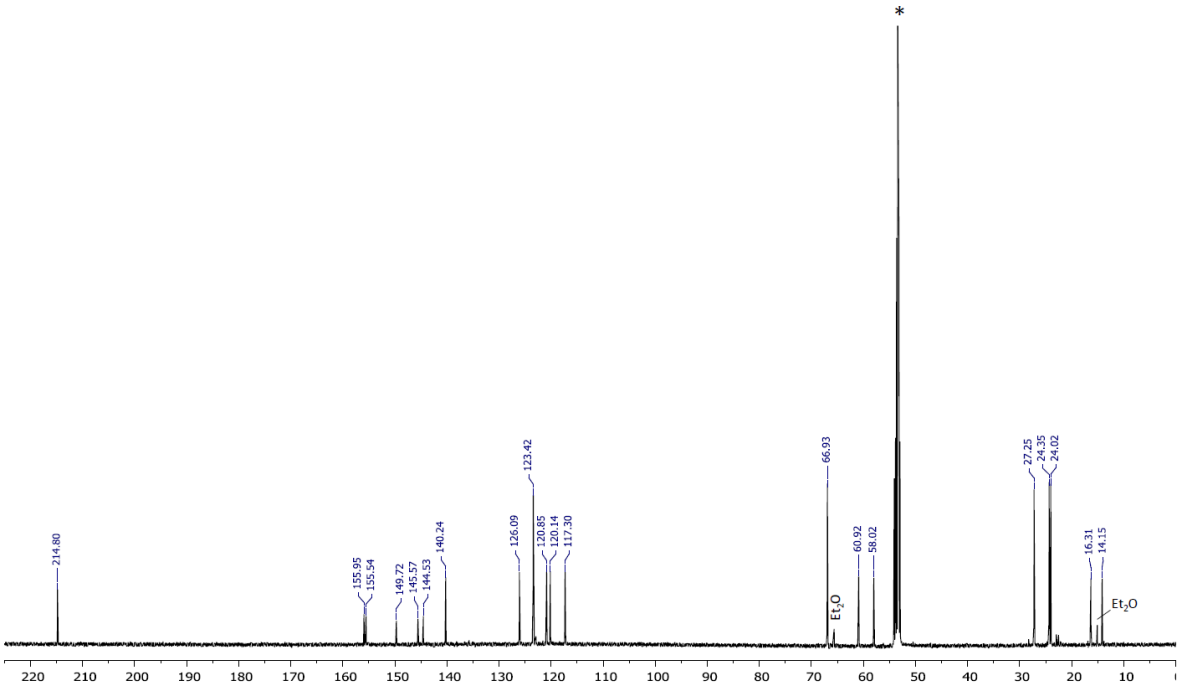

Figure S6. $^{13}C\{^{1}H\}$ NMR of Fe(^{Mor}PDI)(CO)$_2$ (**4**), 125 MHz, CD_2Cl_2.

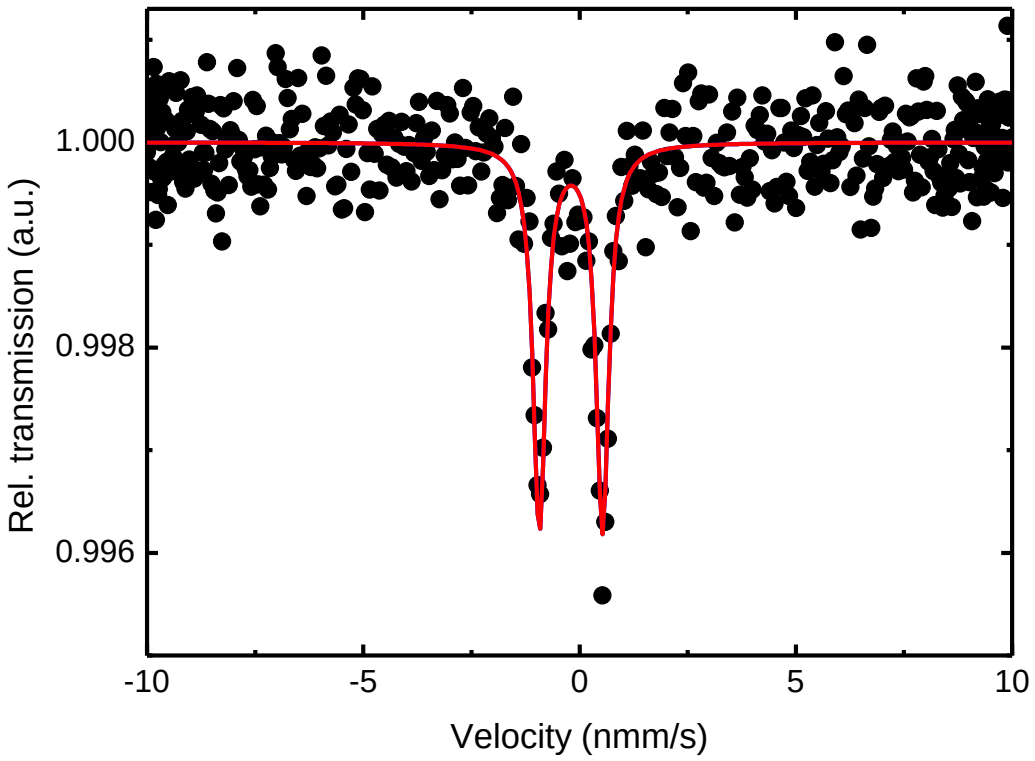

Figure S7. Room temperature zero-field Mössbauer spectrum of Fe(^{Mor}PDI)(CO)$_2$ (**4**); δ = -0.10(1) mm/s, ΔE_Q = 1.46(2) mm/s, Line width, Γ = 0.36(2) mm/s.

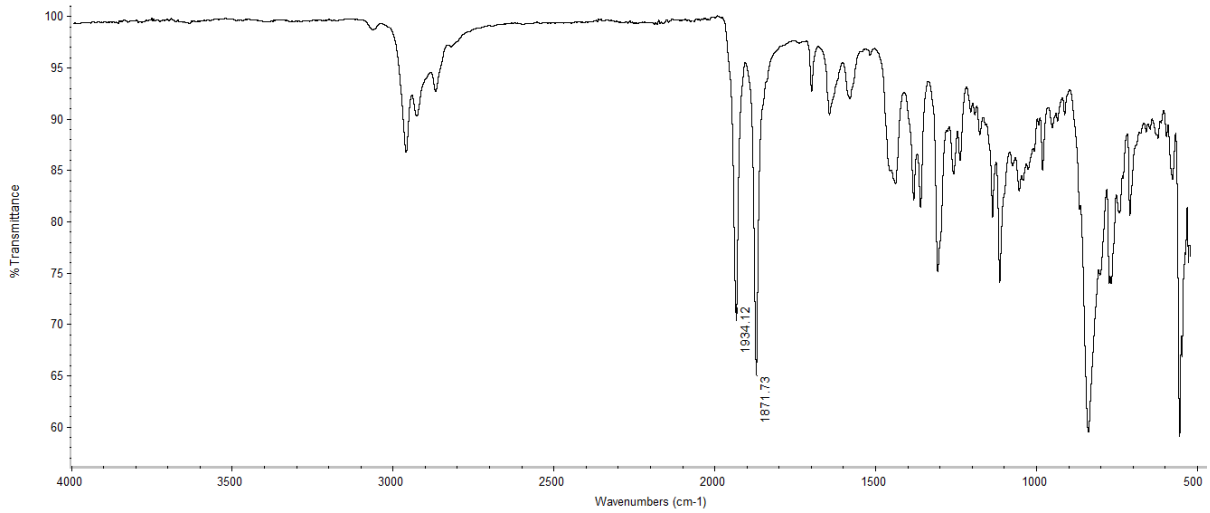

Figure S8. Solid FT-IR ATR spectrum of Fe(^{Mor}PDI)(CO)$_2$ (**4**).

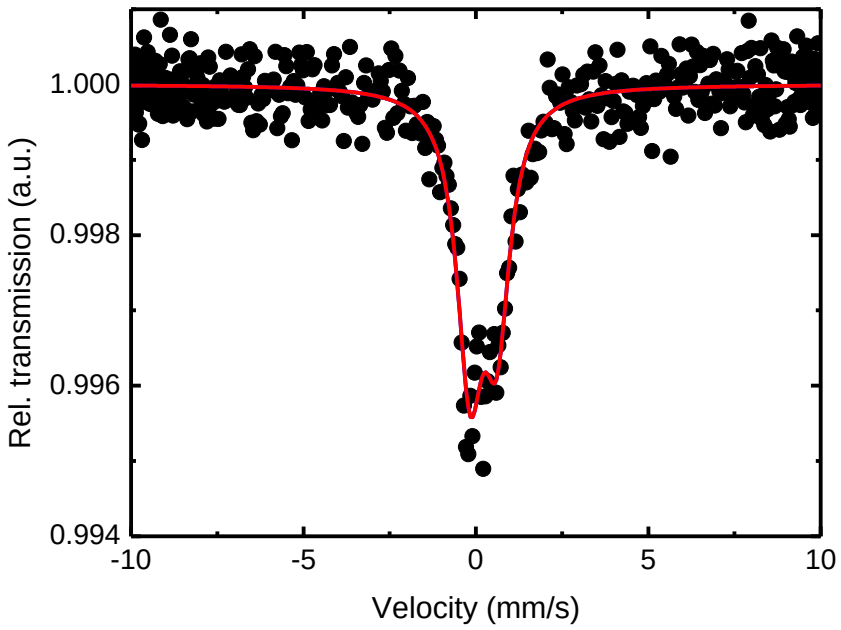

Figure S9. Room temperature zero-field Mössbauer spectrum of [Fe(^{Pyrr}PDI)(NO)$_2$][BPh$_4$] (**5**); δ = 0.32(3) mm/s, ΔE_Q = 0.82(9) mm/s, Line width, Γ = 0.92(5) mm/s.

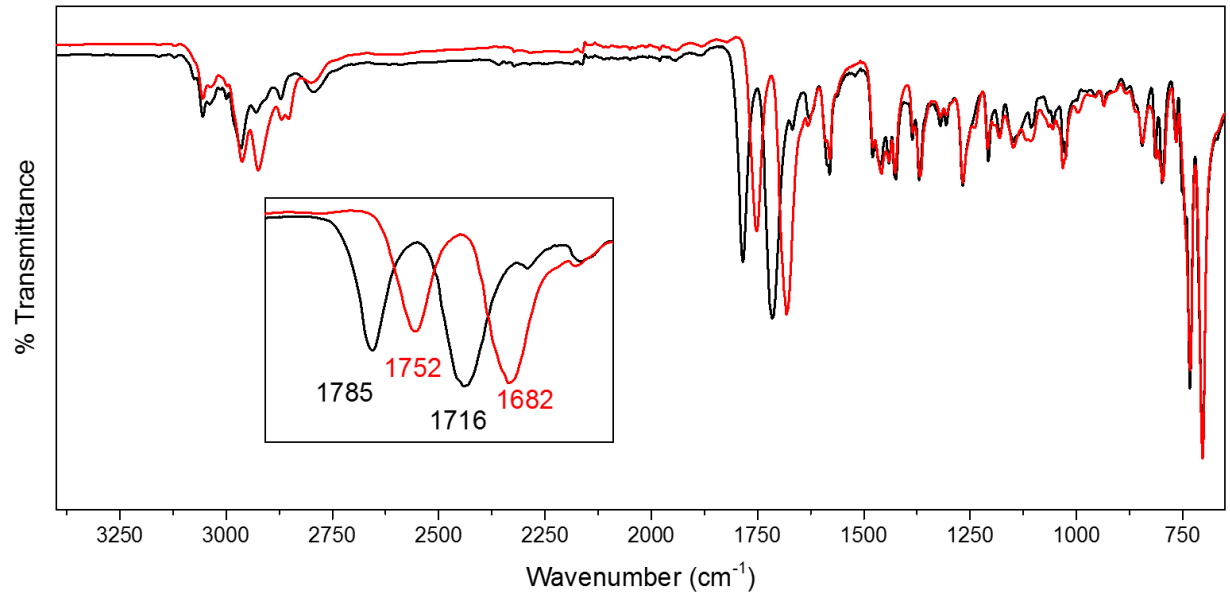

Figure S10. Solid FT-IR ATR spectrum of [Fe(^{Pyrr}PDI)(NO)$_2$][BPh$_4$] (**5**) (black line) and [Fe(^{Pyrr}PDI)(^{15}NO)$_2$][BPh$_4$] (red line). The inset is the ν_{NO} region expanded.

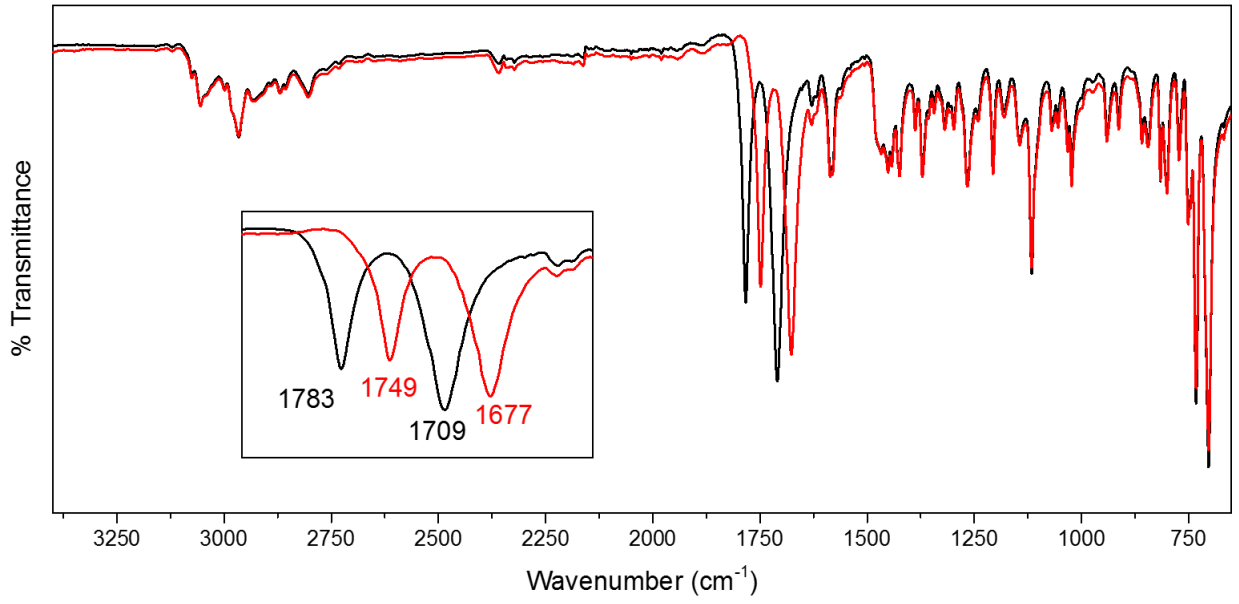

Figure S11. Solid FT-IR ATR spectrum of [Fe(^{Mor}PDI)(NO)$_2$][BPh$_4$] (**6**) (black line) and [Fe(^{Mor}PDI)(^{15}NO)$_2$][BPh$_4$] (red line). The inset is the ν_{NO} region expanded.

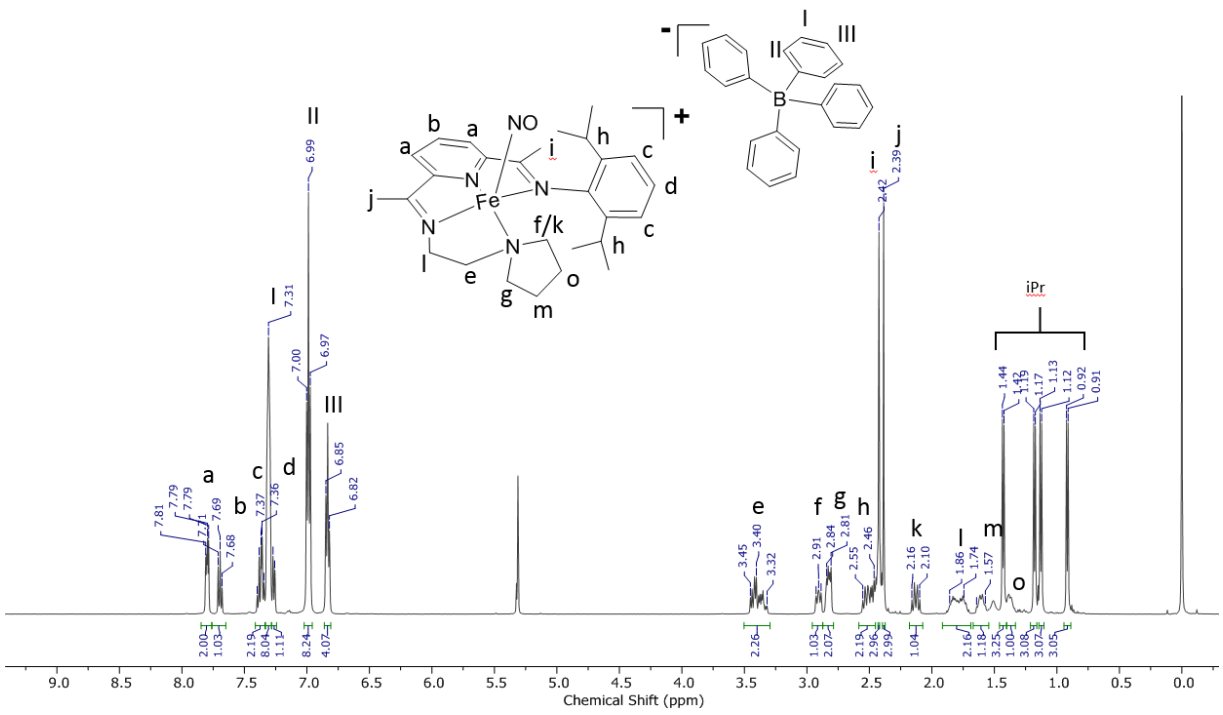

Figure S12. ^{1}H NMR of [Fe(^{Pyrr}PDI)(NO)][BPh$_4$] (**9**), 500 MHz, CD_2Cl_2.

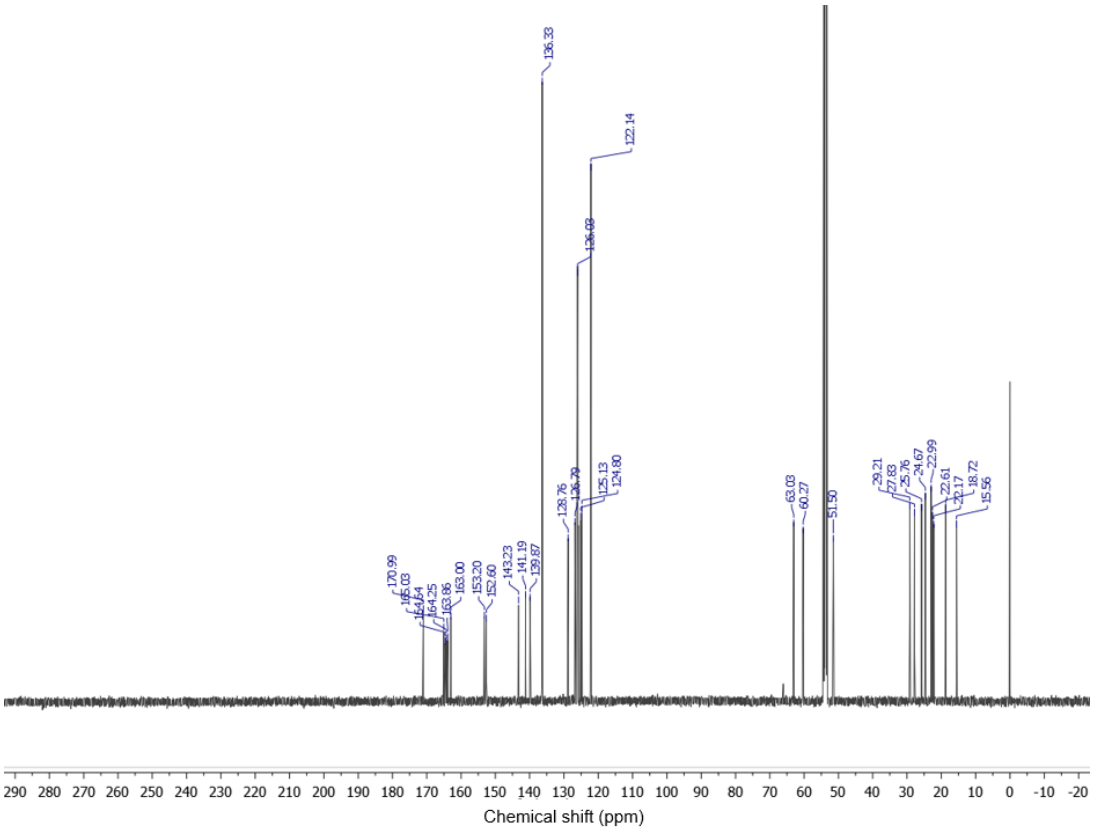

Figure S13. $^{13}C\{^{1}H\}$ NMR of [Fe(^{Pyrr}PDI)(NO)][BPh_4] (**9**), 125 MHz, CD_2Cl_2.

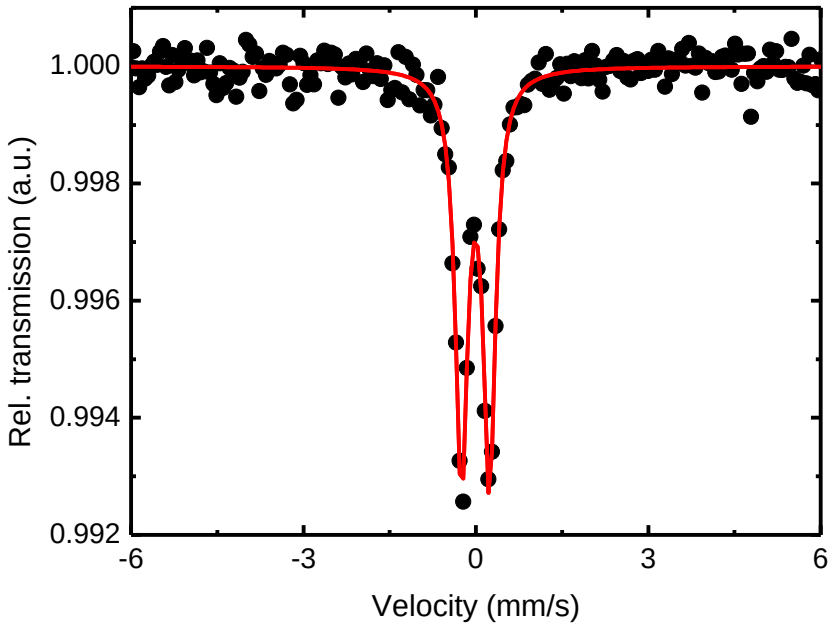

Figure S14. Room temperature zero-field Mössbauer spectrum of [Fe(^{Pyrr}PDI)(NO)][BPh_4] (**9**); δ = 0.094(3) mm/s, ΔE_Q = 0.489(5) mm/s, Line width, Γ = 0.254(7) mm/s.

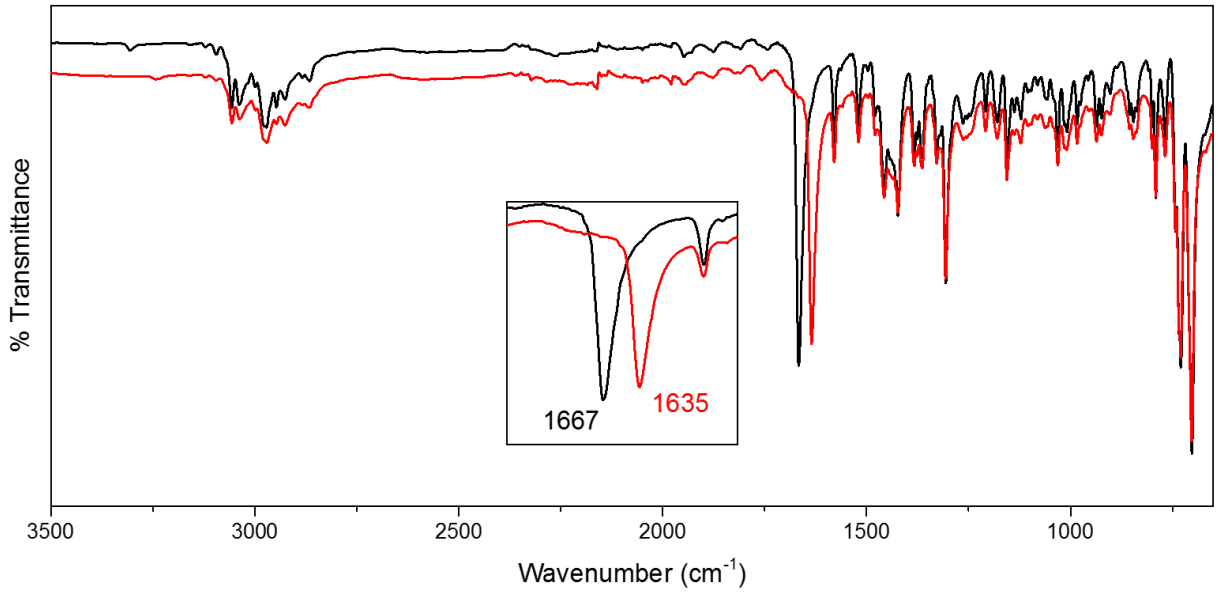

Figure S15. Solid FT-IR ATR spectrum of [Fe(^{Pyrr}PDI)(NO)][BPh$_4$] (**9**) (black line) and [Fe(^{Pyrr}PDI)(^{15}NO)][BPh$_4$] (red line). The inset is the ν_{NO} region expanded.

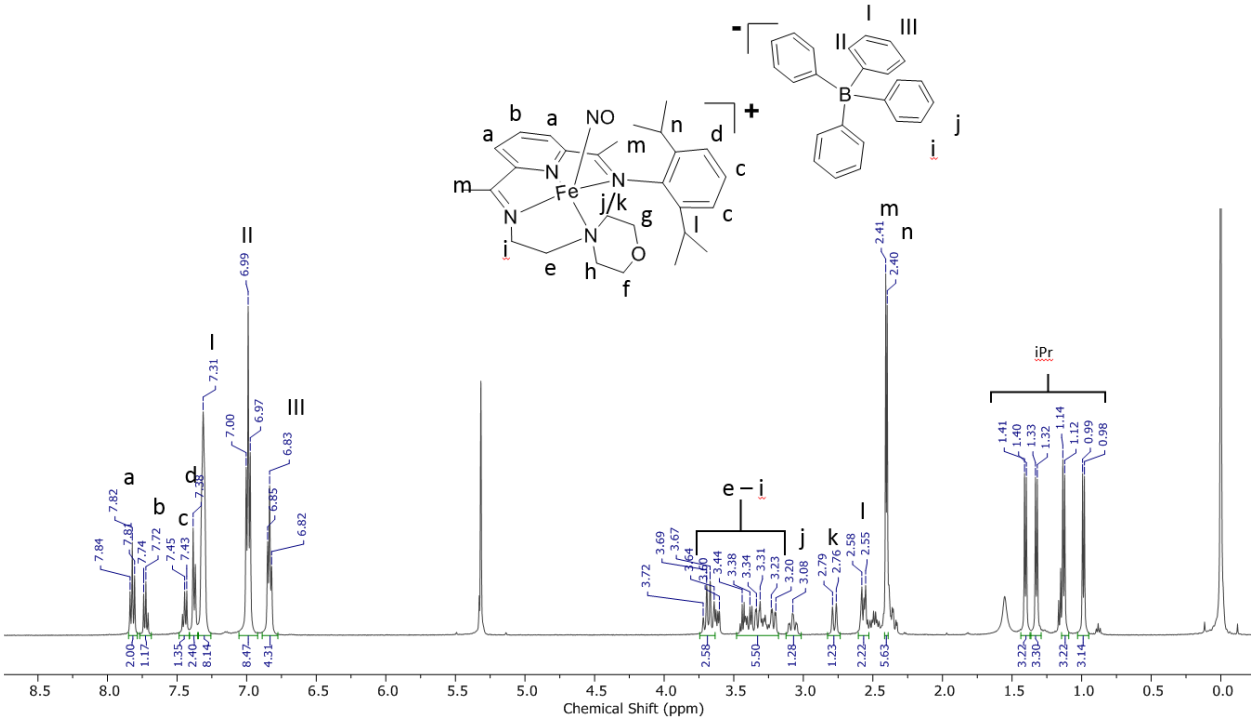

Figure S16. ^{1}H NMR of [Fe(^{Mor}PDI)(NO)][BPh$_4$] (**10**), 500 MHz, CD_2Cl_2.

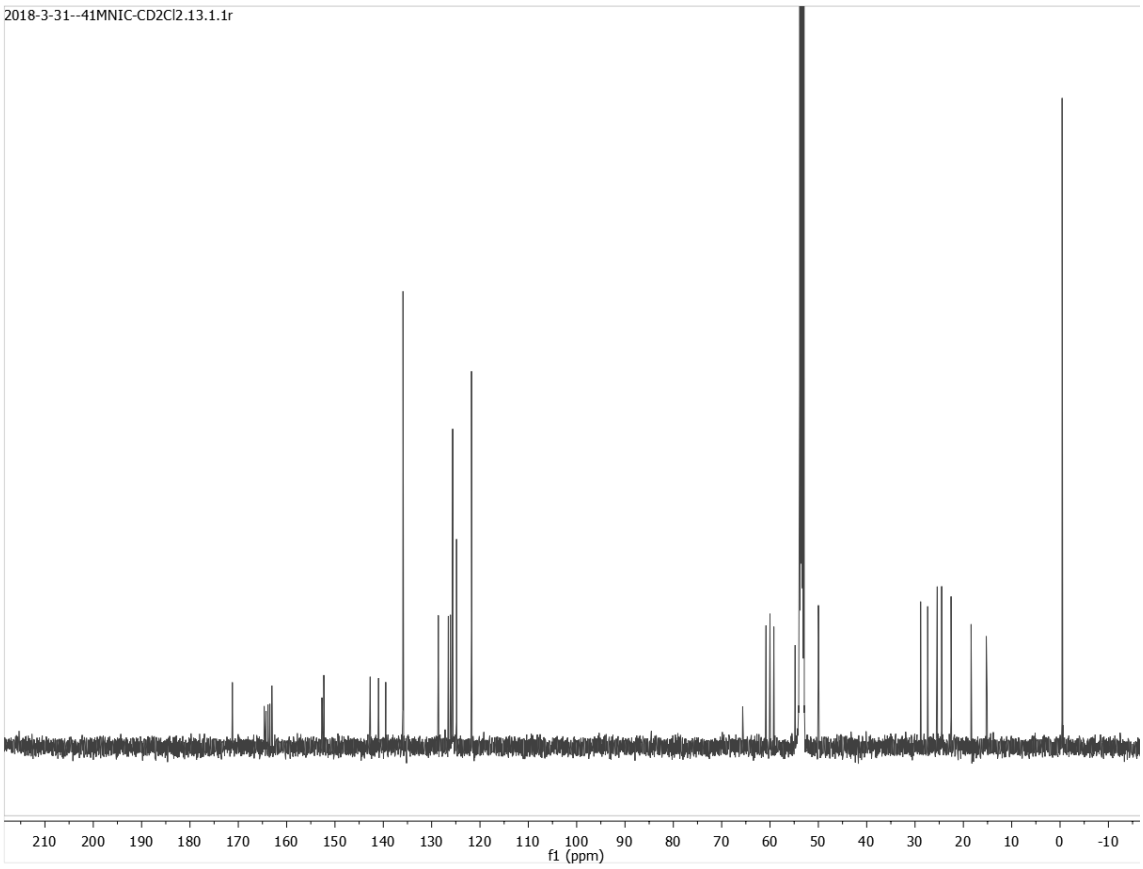

Figure S17. $^{13}C\{^{1}H\}$ NMR of [Fe(^{Mor}PDI)(NO)][BPh_4] (**10**), 125 MHz, CD_2Cl_2.

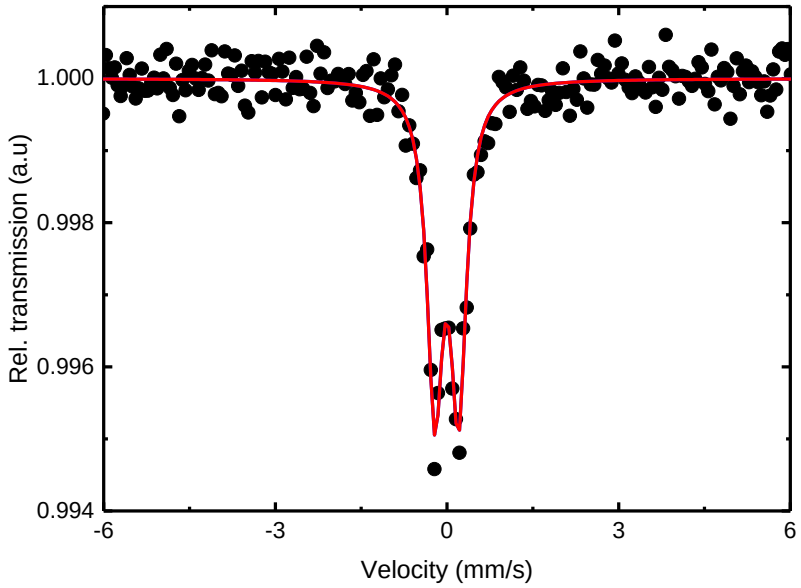

Figure S18. Room temperature zero-field Mössbauer spectrum of [Fe(^{Mor}PDI)(NO)][BPh_4] (**10**); δ = 0.095(5) mm/s, ΔE_Q = 0.415(9) mm/s, Line width, Γ = 0.32(1) mm/s.

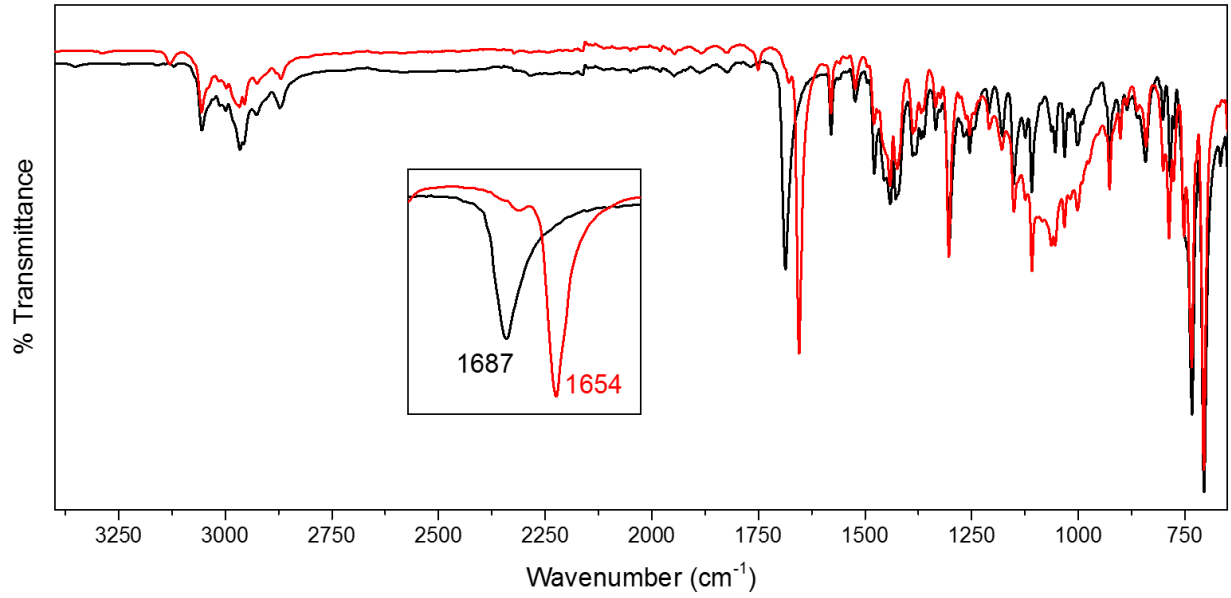

Figure S19. Solid FT-IR ATR spectrum of [Fe(^{Mor}PDI)(NO)][BPh_4] (**10**) (black line) and [Fe(^{Mor}PDI)(^{15}NO)][BPh_4] (red line). The inset is the ν_{NO} region expanded.

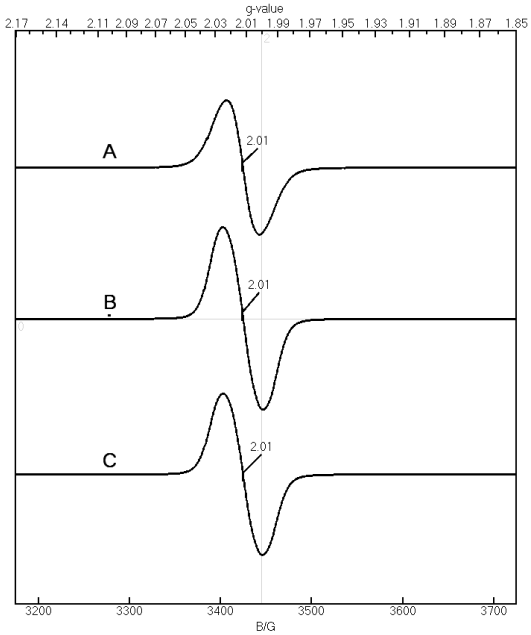

Figure S20. Overlaid EPR Spectra of [Fe(^{Pyrr}PDI)$(NO)_2$][BPh_4] (**5**) (top), [Fe(^{Mor}PDI)$(NO)_2$][BPh_4] (**6**) (middle), and [Fe(didpa)$(NO)_2$][BPh_4] (bottom), 11 K CH_2Cl_2.

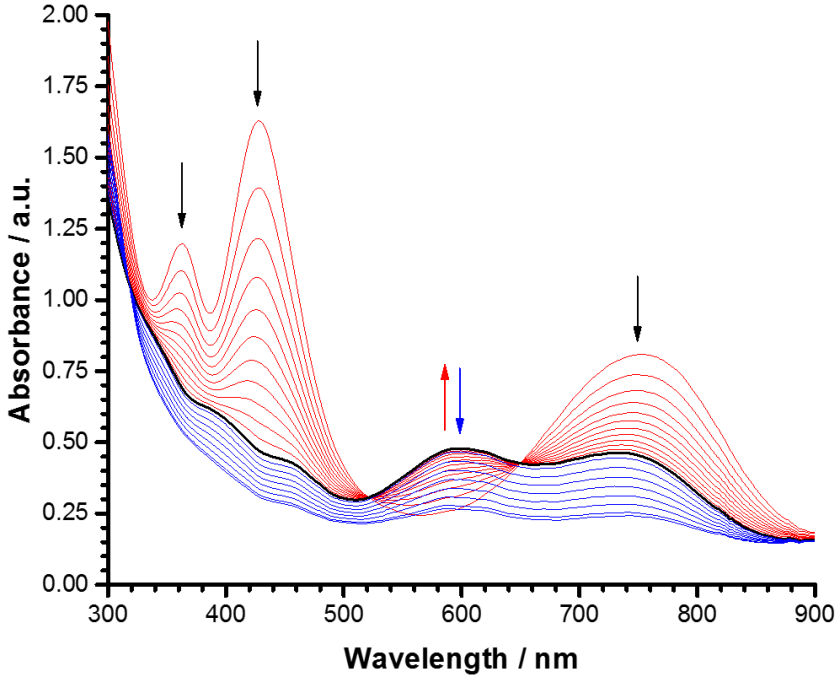

Figure S21. Stacked UV-Vis spectra of Fe(^{Pyrr}PDI)(CO)$_2$ (**3**), TBANO$_2$ and [HNEt$_3$][BPh$_4$], 10 mins between each scan demonstrating the disappearance of Fe(^{Pyrr}PDI)(CO)$_2$ (**3**) with concomitant appearance of [Fe(^{Pyrr}PDI)(NO)][BPh$_4$] (**9**). Compound **9** peaks at 110 mins (black trace) and begins to disappear with the concomitant formation of [Fe(^{Pyrr}PDI)(NO)$_2$][BPh$_4$] (**5**). The black trace at 110 mins also corresponds to the inflection point in the global kinetic plot (blue line, Figure S22). Isosbestic points are located at 522 nm and 650 nm.

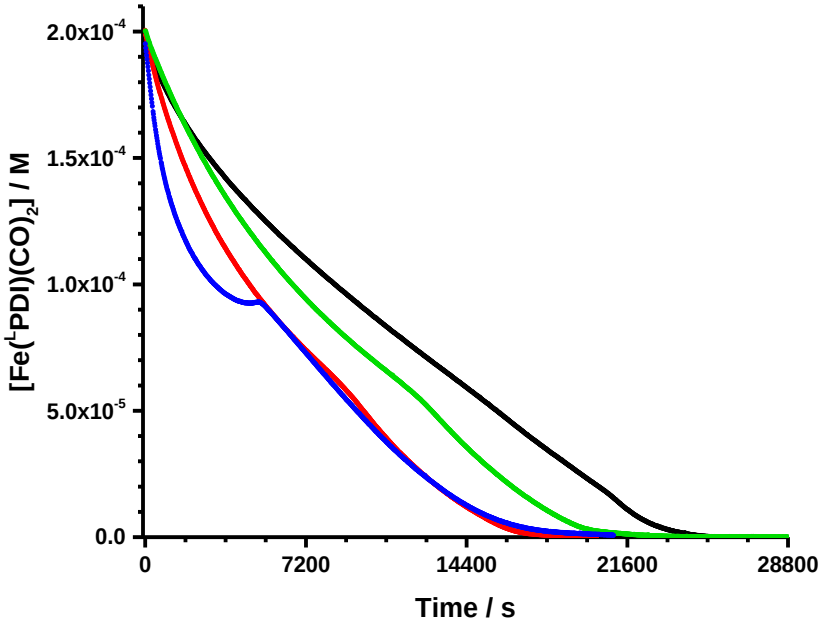

Figure S22. Overlaid kinetics runs for the reduction of TBANO$_2$ by selected Fe(PDI)(CO)$_2$ species and 4 equiv. [HNEt$_3$][BPh$_4$]. Black line = Fe(^{MeO}PDI)(CO)$_2$ (**7**); green line = Fe(^{Mor}PDI)(CO)$_2$ (**4**); red line = Fe(didpa)(CO)$_2$ (**8**); blue line = Fe(^{Pyrr}PDI)(CO)$_2$ (**3**).

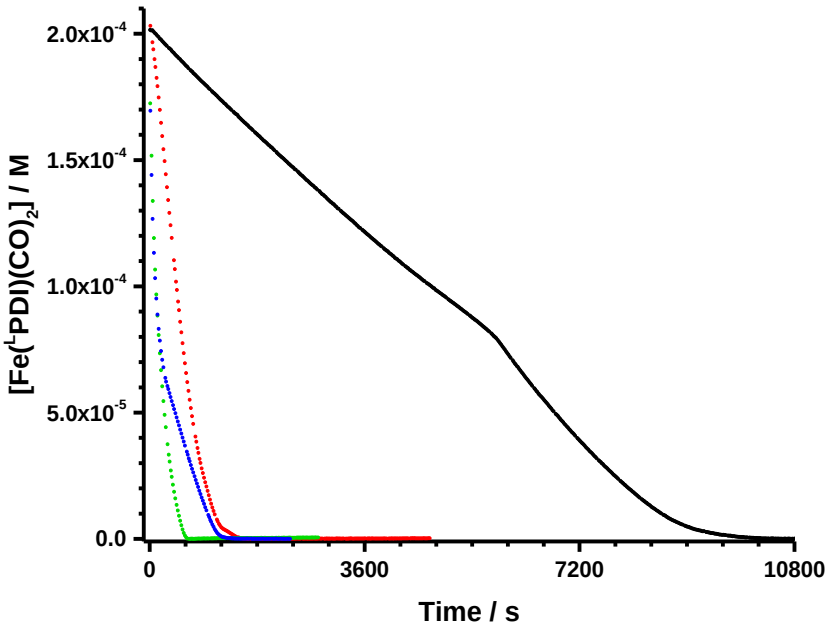

Figure S23. Overlaid kinetics runs for the reduction of $TBANO_2$ by selected $Fe(PDI)(CO)_2$ species and 4 equiv. [HLut][BPh_4]. Black line = $Fe(^{MeO}PDI)(CO)_2$ (**7**); green line = $Fe(^{Mor}PDI)(CO)_2$ (**4**); red line = Fe(didpa)$(CO)_2$ (**8**); blue line = $Fe(^{Pyrr}PDI)(CO)_2$ (**3**).

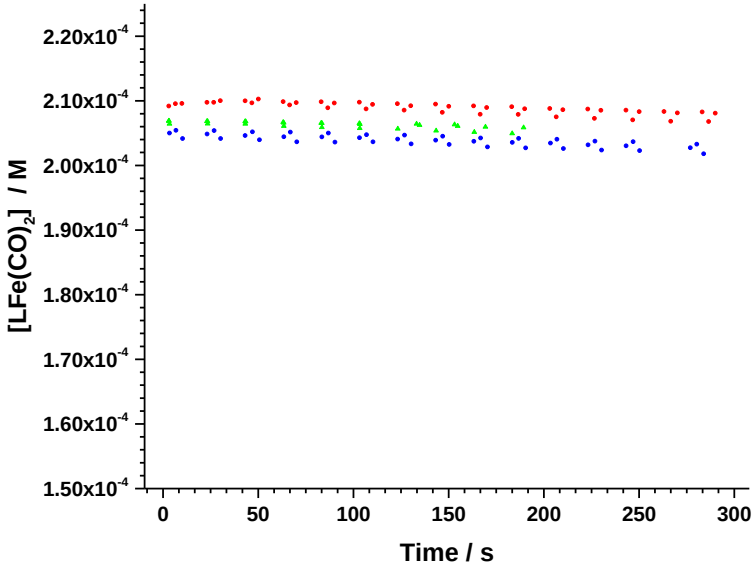

Figure S24. Overlaid [ ] vs. time curves for $Fe(^{MeO}PDI)(CO)_2$ (**7**) after injection of no acid (green), $[HNEt_3]^+$ (blue line), and $[HLut]^+$ (red line), illustrating no side reactions of the $Fe(^{MeO}PDI)(CO)_2$ with H^+. These reactions contain no $TBANO_2$.

Table of Compiled Kinetic Data. K1 (black) = Fe(^{MeO}PDI)(CO)$_2$ (**7**); K2 (red) = Fe(didpa)(CO)$_2$ (**8**); K3 (green) = Fe(^{Mor}PDI)(CO)$_2$ (**4**); K4 (blue) = Fe(^{Pyrr}PDI)(CO)$_2$ (**3**).

[NEt$_3$H][BPh$_4$]

	Intercept		Slope		Statistics	Average Rate	Std. Dev.	Rel to K1
	Value	Standard Error	Value	Standard Error	Adj. R-Square			
K1	1.96E-04	5.10E-08	-2.23E-08	1.39E-10	0.99923	-2.11E-08	1.59856E-09	1.00
	1.91E-04	1.02E-07	-1.93E-08	2.77E-10	0.9959			
	1.90E-04	9.58E-08	-2.17E-08	2.59E-10	0.99717			
K2	1.98E-04	7.27E-08	-3.52E-08	2.01E-10	0.99934	-3.97E-08	9.01066E-09	1.88
	1.94E-04	5.18E-07	-5.01E-08	1.44E-09	0.98381			
	1.93E-04	1.36E-07	-3.38E-08	3.74E-10	0.99756			
K3	2.00E-04	4.76E-08	-2.28E-08	1.30E-10	0.99935	-2.30E-08	1.27609E-09	1.09
	2.01E-04	4.84E-08	-2.19E-08	1.31E-10	0.99928			
	2.00E-04	7.76E-08	-2.44E-08	2.09E-10	0.99854			
K4	1.94E-04	3.48E-07	-6.96E-08	9.55E-10	0.99625	-7.07E-08	9.22778E-10	3.35
	1.92E-04	4.11E-07	-7.12E-08	1.12E-09	0.9951			
	1.95E-04	3.78E-07	-7.12E-08	1.02E-09	0.99594			

[LutH][BPh$_4$]

	Intercept		Slope		Statistics	Average Rate	Std. Dev.	Rel to K1
	Value	Standard Error	Value	Standard Error	Adj. R-Square			
K1	2.03E-04	8.00E-08	-2.37E-08	3.46E-10	0.99597	-2.52E-08	2.29906E-09	1.19
	2.04E-04	2.96E-08	-2.40E-08	1.30E-10	0.99944			
	2.03E-04	1.18E-07	-2.78E-08	5.03E-10	0.99383			
K2	2.07E-04	4.99E-07	-2.09E-07	4.22E-09	0.99633	-2.12E-07	8.1497E-09	10.06
	2.06E-04	2.30E-07	-2.07E-07	2.06E-09	0.99911			
	2.05E-04	2.75E-07	-2.22E-07	2.40E-09	0.99895			
K3	1.81E-04	2.84E-06	-8.69E-07	5.48E-08	0.98429	-8.45E-07	3.93238E-08	40.01
	1.83E-04	3.18E-06	-8.66E-07	5.78E-08	0.9824			
	1.79E-04	2.67E-06	-7.99E-07	4.61E-08	0.98683			
K4	1.74E-04	4.63E-06	-8.36E-07	8.93E-08	0.9559	-8.11E-07	2.20153E-08	38.42
	1.73E-04	4.00E-06	-7.95E-07	7.30E-08	0.96715			
	1.74E-04	4.94E-06	-8.02E-07	8.57E-08	0.95584			

Control Experiments with CoTPP. The NO trapping experiment with $TBANO_2$ and [HLut][BPh_4] was performed following literature procedures.4,5 A small vial containing 2 mL of CoTPP solution in DCM (15.0 µM, 2.98 × 10-8 mol) was placed in a 20 mL scintillation vial charged with 2.15 µL of $TBANO_2$ in MeCN (32.0 mM, 6.86 × 10-8 mol) and a stir bar. The scintillation vial was sealed with a septum and set on a stir plate. A solution of [HLut][BPh_4] in MeCN (0.15 mL, 1.83 mM, 2.75 × 10-7 mol) was injected into the scintillation vial. The mixture was gently stirred for 60 minutes. The UV-Vis spectrum of the resulting CoTPP/DCM solution in the small vial was recorded and compared to the initial spectrum. The ratios of CoTPP:$TBANO_2$:H^+ were adjusted to 1:1:2 and 1:1:4. These results show no appreciable NO production from $[Hlut]^+$ + $TBANO_2$ in CH_3CN during the timescale of the reaction.

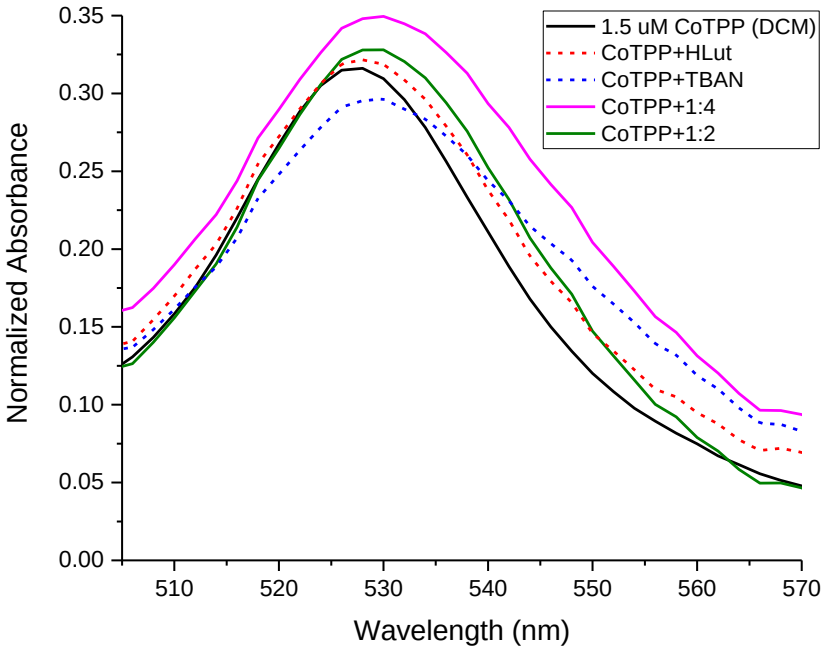

Figure S25. UV-Vis spectra of 1.5 µM Co(TPP) in CH_3CN (black line), Co(TPP) + 1 equiv. $[Hlut]^+$ (red dash), Co(TPP) + 1 equiv. $TBANO_2$ (blue dash), Co(TPP) + 1 equiv. $TBANO_2$ +2 equiv $[Hlut]^+$ (green line), and Co(TPP) + 1 equiv. $TBANO_2$ +4 equiv $[Hlut]^+$ (green line).

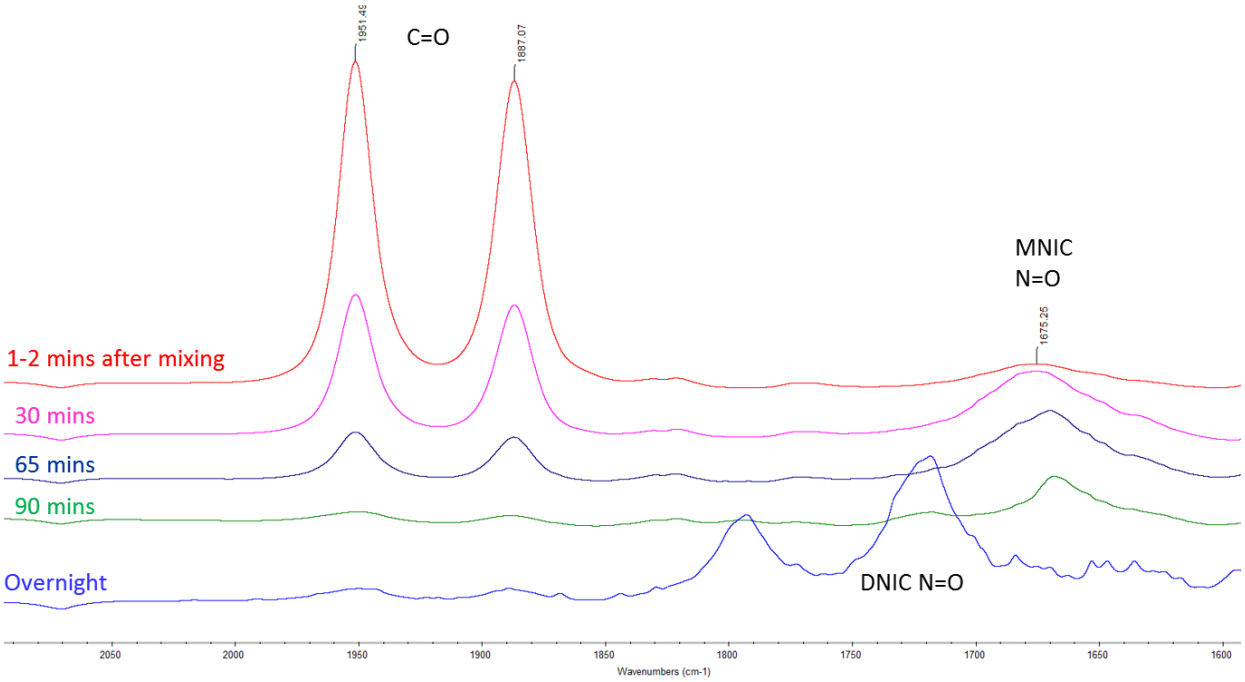

Figure S26. Liquid FTIR spectra (CH_3CN) of the reaction between $Fe(^{Pyrr}PDI)(CO)_2$ (**3**) , 2 eq. $TBANO_2$ and 4 eq $[HEt_3N][BPh_4]$.

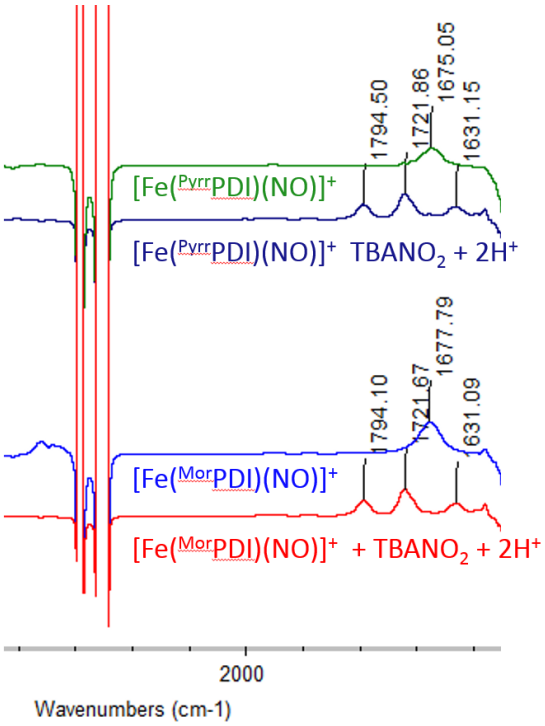

Figure S27. Liquid FTIR spectra (CH_3CN) of the reactions between $[Fe(^{Pyrr}PDI)(NO)]^+$ (**9**), 1 eq. $TBANO_2$ and 2 eq $[HEt_3N][BPh_4]$ (top) and $[Fe(^{Mor}PDI)(NO)]^+$ (**10**), 1 eq. $TBANO_2$ and 2 eq $[HEt_3N][BPh_4]$ (bottom). These reactions show the conversion between the MNICs and DNICs by adding one 1 eq. $TBANO_2$ and 2 eq $[HEt_3N][BPh_4]$.

Benchmarking of exchange-correlation (XC) functionals against crystallographic data

Selection of an appropriate exchange-correlation (XC) functional for DFT analysis of electronic structure in complexes **5** and **9** was informed by geometry optimizations employing six XC functionals encompassing the major classes employed in computational studies of related complexes. BP86 was chosen as a representative of GGA functionals; TPSSh and M06-L represent the spectrum of functionals in the meta-GGA family; B3LYP and PBE0 represent global hybrid functionals; and ωB97X-D represents the range-separated hybrid functional family. The geometry of complexes **5** and **9** was optimized with each functional using the TZVP(-f) basis set, and the root-mean-square deviation (RMSD) of the optimized structure to the experimentally determined crystal structure was used to select an XC functional for analysis of the electronic structure.

We find a dramatic difference between pure and hybrid XC functionals for MNIC **9**. The hybrid functionals present both a broken-symmetry BS(2,2) solution and a restricted BS(0,0) solution; in contrast, the BS(2,2) solution could not be converged with the pure functionals. This qualitative difference between pure and hybrid functionals has been observed in computational studies of related iron nitrosyls.[1] Following the conclusions of Ref. 2 and related work[3], we anticipate that the BS(2,2) ground state predicted by the hybrid functionals is more consistent with multireference (e.g. RASSCF) treatments of iron complexes with redox-active ligands.[4] We therefore adopt the PBE0 description of the MNIC **9** because it is the hybrid functional for which the optimized geometry shows the smallest RMSD versus the crystal structure. In contrast, pure and hybrid XC functionals' descriptions of the DNIC are qualitatively similar, and the functional with smallest geometry RMSD is BP86 (Table S3). We therefore adopt the BP86 functional for analysis of DNIC **5**. Finally, given the previously established role of a BS configuration in complex **3**, we located both BS(0,0) and BS(2,2) solutions with the ωB97X-D3 functional.

1) Hopmann, K. H.; Conradie, J.; Ghosh, A. Broken-Symmetry DFT Spin Densities of Iron Nitrosyls, Including Roussin's Red and Black Salts: Striking Differences between Pure and Hybrid Functionals. *J. Phys. Chem. B* **2009**, *113*, 10540.

2) Kumar, M.; Dixon, N. A.; Merkle, A. C.; Zeller, M.; Lehnert, N., Papish, E. T. Hydrotris(triazolyl)borate Co mplexes as Functional Models for Cu Nitrite Reductase: The Electronic Influence of Distal Nitrogens. *Inorg. Chem.*, **2012**, *51*, 7004.

3) Roos, B. O.; Veryazov, V.; Conradie, J.; Taylor, P. R.; Ghosh, A. Not Innocent: Verdict from Ab Initio Multiconfigurational Second-Order Perturbation Theory on the Electronic Structure of Chloroiron Corrole. *J. Phys. Chem. B* **2008**, *112*, 14099.

4) Ortuño, M. A.; Cramer, C. J. Multireference Electronic Structures of Fe–Pyridine(diimine) Complexes over Multiple Oxidation States. *J. Phys. Chem. A* **2017**, *121*, 5932.

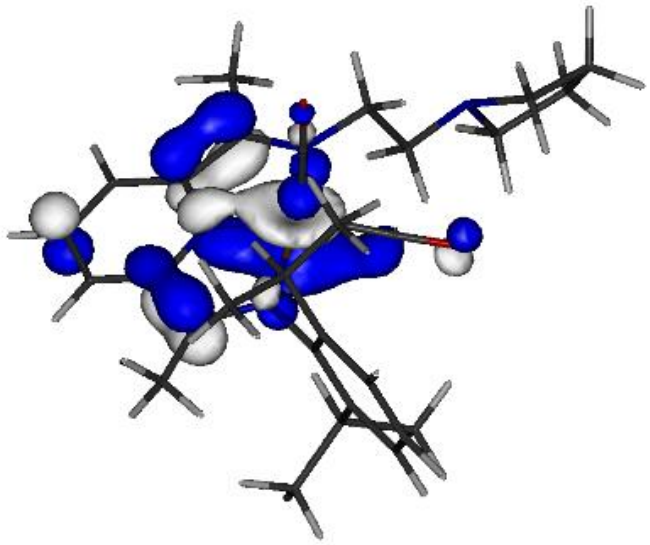

Figure S28. HOMO of the BS(0,0) solution for Fe(^{Pyrr}PDI)(CO)$_2$ (**3**).

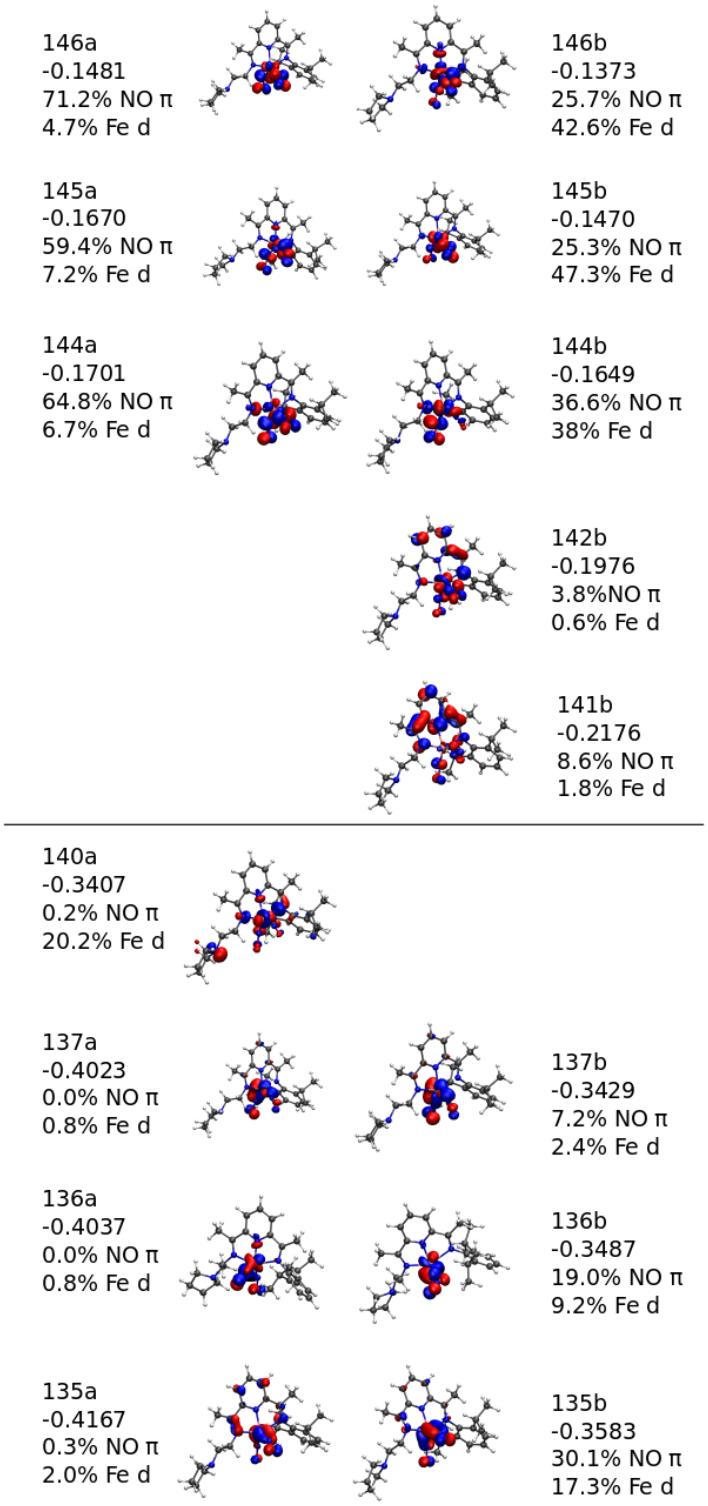

Figure S29. Frontier MOs of the S = ½ unrestricted KS solution for [Fe(^{Pyrr}PDI)$(NO)_2]^+$ (**5**).

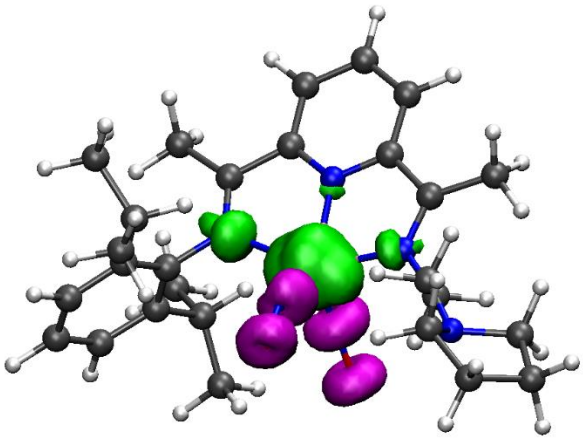

Figure S30. Spin density of [Fe(^{Pyrr}PDI)$(NO)_2]^+$ (**5**).

Table S1. Selected bond lengths (Å) and angles (°) of Fe(PDI) complexes

	5	**5^{KS}**	**9**	**9$^{(2,2)}_{PBE0}$**	**9$^{(0,0)}_{PBE0}$**	**9$^{(2,2)}_{ωB97X-D3}$**	**9$^{(0,0)}_{ωB97X-D3}$**
C(2)-N(1)	1.285(2)	1.300	1.315(2)	1.302	1.302	1.294	1.292
C(8)-N(3)	1.283(2)	1.294	1.313(2)	1.314	1.314	1.309	1.294
C(2)-C(3)	1.488(3)	1.476	1.453(2)	1.450	1.451	1.485	1.463
C(7)-C(8)	1.488(3)	1.484	1.439(2)	1.432	1.432	1.435	1.456
Fe(1)-N(1)	2.216(2)	2.102	2.031(1)	2.060	2.059	2.071	2.043
Fe(1)-N(2)	2.080(1)	2.039	1.830(2)	1.839	1.839	1.849	1.852
Fe(1)-N(3)	2.138(2)	2.306	1.894(1)	1.899	1.898	1.913	1.920
Fe(1)-N_{pyr}(4)			2.066(1)	2.101	2.101	2.113	2.149
Fe(1)-N(5)(O)	1.693(2)	1.676	1.677(2)	1.747	1.748	1.754	1.639
Fe(1)-N(6)(O)	1.696(2)	1.687					
N(5)-O(1)	1.170(3)	1.167	1.182(2)	1.167	1.167	1.168	1.165
N(6)-O(2)	1.173(3)	1.170					
Fe(1)-N(5)-O(1)	161.9(2)	163.6	150.9(2)	147.5	147.3	152.5	143.3
Fe(1)-N(6)-O(2)	160.4(2)	157.5					

Table S2. Selected atomic Mulliken spin populations on DNIC (5) at the BP86/TZVP(-f) level of theory

Atom	Spin pop.
Fe	+1.27
N(5)	−0.12
O(1)	−0.13
N(6)	−0.10
O(2)	−0.11

Table S3. RMSD of DFT-optimized geometries relative to crystallographic data for DNIC (5) and MNIC (9)

Functional	Family	RMSD (DNIC 5, Å)	RMSD (MNIC 9, Å)
BP86	GGA	0.5148	0.2315[†]
TPSSh	meta-GGA	0.7803	0.2296[†]
M06-L	meta-GGA	4.2529[*]	0.7895[†]
B3LYP	global hybrid	0.6695	0.2720
PBE0	global hybrid	0.7042	0.2521
ωB97X-D3	range-separated hybrid	0.7812	0.3525

[*]Fe center escaped from PDI binding pocket during M06-L geometry optimization of DNIC **5**.

[†]Converged to BS(0,0) solution instead of targeted BS(2,2) solution.

BS(0,0) optimized geometry of Fe(^{Pyrr}PDI)(CO)$_2$ (**3**) at the ωB97X-D3/def2-TZVP(-f) level

```
Energy of BS(0,0) at this geometry = -2761.338603 Hartree
Energy of BS(2,2) at this geometry = -2761.339834 Hartree
  Fe   4.09051714037457      8.65159215488899     10.85530380826677
  O    4.57063245796120      5.91255174216392     11.82980151264440
  O    4.29791321618191     10.17636547122213     13.32338871086446
  N    5.99869469897226      9.02378905213074     10.50176794480153
  N    2.13002106464831      8.53922971663404     10.51398684332626
  N    3.93947683976021      9.75368867709404      9.40627482420458
  N    9.48803811696460      8.38377145021111     10.83479693455242
  C    2.69670943194660     10.12289608997700      8.94837810991978
  C    0.87736544074522      6.43847739323459     10.41177207456077
  C    5.06524821203360     10.33988901635288      8.87839628982285
  C    6.24922528554712      9.87679588651586      9.53958152023985
  C    1.67243842112783      9.37996603884067      9.60645146450934
  C    1.61134565806365      5.98882633012845      9.15619535361232
  H    2.36134441963940      6.74423248648644      8.91980638826844
  C    1.17869617270951      7.63145830734699     11.09507707659330
  C    2.57617951091310     11.09015812730813      7.96075630910327
  H    1.59743964181706     11.39507079377645      7.61193057078670
  C   -0.10236339348316      5.60716813325428     10.93872603184393
  H   -0.35340573748625      4.69099443295788     10.41636661317322
  C    4.34318044667070      6.96400361921712     11.43911901201807
  C    0.55583634745807      7.93508894400052     12.31464043732663
  C    7.07316425444918      8.57708173755278     11.39529732024050
  H    6.59548987274301      8.00459412187124     12.18683932777593
  H    7.53098691083861      9.44929653730940     11.87162562303274
  C    8.19157754788024      7.73511519297729     10.75296410843773
  H    8.21948964031674      6.74969748128072     11.24199321322040
  H    7.94924162427469      7.55665621536407      9.70360195257046
```

C	4.16476228353427	9.53552425751853	12.38363018272825
C	0.95338423998614	9.13445219888719	13.15326305072185
H	1.64507190525626	9.73537602413310	12.56384396626284
C	7.61432881435456	10.35448588633255	9.14206045760305
H	8.31848730441940	10.31270137270996	9.97187717649819
H	7.57810256572288	11.37104509445427	8.75251271750577
H	8.01725204622197	9.72013609419617	8.34870822734133
C	4.96445983735911	11.28796242396581	7.87840569152628
H	5.85832931908121	11.73350051271210	7.46130600465476
C	3.71047893487376	11.67398025221813	7.41439794439162
H	3.62116240531151	12.42620501873199	6.64312663814536
C	0.21628413072219	9.53526064373230	9.29069269710171
C	-0.41159808316636	7.06315877753965	12.80249204228105
H	-0.89984864931582	7.28897084943719	13.74320860276156
C	10.43120226627845	8.02689535099292	9.78659422786568
H	10.09730711085178	8.44857276360049	8.83465759114768
H	10.52084430796426	6.93492054412335	9.65577774708735
C	2.33982421199130	4.66236908405021	9.40666572432448
H	2.99888586375720	4.71948481372761	10.27084086191871
H	2.94169603771396	4.38856222610629	8.53754508303203
H	1.62815887937773	3.85354626091193	9.58769006145386
C	-0.75365699623981	5.91272235947698	12.11975087969823
H	-1.50578520923147	5.24378835898446	12.51980130382255
C	1.68403717152884	8.66472388252327	14.41745977024248
H	1.01292314874428	8.08529417065256	15.05727499727441
H	2.06033869728613	9.51344121753809	14.99027069285659
H	2.53097289827108	8.02369826177278	14.16843250896749
C	-0.22247609287749	10.03127401196144	13.53511652777479
H	-0.76428604743887	10.39947909712668	12.66205477971856
H	0.14842128596349	10.89280201430221	14.09476194671575
H	-0.93617572427094	9.50465746651072	14.17357486035162
C	10.19375625496869	8.17793763352469	12.09067111076577
H	10.19826521141619	7.10964830452735	12.37161811798012
H	9.70222263276656	8.72025859736595	12.90106117283437
C	11.62212387460513	8.66829299308983	11.81059044823503
H	11.77446473271860	9.67883491261436	12.18921315319164
H	12.35582017269346	8.02957989154813	12.30065593355290
C	0.68816373936113	5.82505610197604	7.94577390085930
H	-0.09558523194970	5.09106034863416	8.14600315174127
H	1.26007981522666	5.46465956830105	7.08712632252982
H	0.19794558121331	6.75909329856146	7.66320708238851
C	11.75357767851634	8.62681436635326	10.27175140218829
H	11.88143888932504	9.63243362844010	9.87077626795715
H	12.60782990119371	8.03720211006799	9.94145783899821
H	0.05289871902882	10.31517555551964	8.55117264162670
H	-0.34692483916876	9.79283695669467	10.18930503519945
H	-0.20652923901424	8.60674929175252	8.90491208045892

BS(2,2) optimized geometry of Fe(^{Pyrr}PDI)(CO)$_2$ (**3**) at the ωB97X-D3/def2-TZVP(-f) level

Energy of BS(0,0) at this geometry = -2761.337631 Hartree
Energy of BS(2,2) at this geometry = -2761.340464 Hartree

Fe	4.09267631360791	8.63061473856412	10.86865511559140
O	4.57945604557408	5.88751796911835	11.85282567491503

O	4.30155342062226	10.20649409386654	13.33994568133027
N	6.01334135849435	9.01679795341838	10.49719765059442
N	2.12407896144007	8.52862971137113	10.52695333931846
N	3.93494537984639	9.75697803391144	9.40373227315774
N	9.50718152855913	8.39508841247760	10.80945373827437
C	2.69053722115458	10.11640834246317	8.95539897384764
C	0.86896839419008	6.42939905308470	10.43400595431539
C	5.05459110963361	10.33267252183471	8.87381228726934
C	6.25094309938154	9.86224368127894	9.53652688959330
C	1.67048033188091	9.37265113645353	9.61738326306205
C	1.60294544165089	5.97390289562724	9.18082226370442
H	2.35604160309754	6.72617599235369	8.94445857446285
C	1.17098938707968	7.62662177145728	11.10947048998710
C	2.56807794987552	11.08421005585879	7.96038759603524
H	1.58960113097362	11.39041006185737	7.61206634094734
C	-0.11174289323576	5.60169729363835	10.96468711064060
H	-0.36326651486336	4.68279399821814	10.44730883849721
C	4.34991727465213	6.93873678313782	11.46133807631877
C	0.54655644738383	7.93738392401911	12.32671602533263
C	7.09357113394225	8.56817635275861	11.38297825224585
H	6.61952393792596	7.98920058685961	12.17165693577130
H	7.54630490592949	9.44099703504602	11.86258649367661
C	8.21525576680965	7.73635000853428	10.73302242553926
H	8.25314790309286	6.75110867766514	11.22127755434252
H	7.96974213323369	7.55643004619777	9.68459302171933
C	4.17069535156032	9.54650624402707	12.41409392865171
C	0.94256949957857	9.14354416551367	13.15641817477904
H	1.63694842700206	9.73812468620698	12.56341958728312
C	7.60757735480241	10.34430533094524	9.11760685484146
H	8.33312471465077	10.27921974654414	9.92722489355065
H	7.56513332245489	11.36862871611529	8.74980884445549
H	7.98163555747024	9.72501023083648	8.29869342511663
C	4.96244782008454	11.27409533731650	7.87381673471471
H	5.85496277646922	11.71655138466427	7.45165323190461
C	3.69918591225114	11.66111521887042	7.41171960641617
H	3.60974386087736	12.41090564416296	6.63791889860459
C	0.21451531253444	9.52857365008349	9.30012127678677
C	-0.42173748646143	7.06915861687022	12.81926316849423
H	-0.91085763599765	7.30125801706359	13.75804961824068
C	10.45043260344756	8.04115810197539	9.75978355176890
H	10.11399725832953	8.46157972329814	8.80813938602656
H	10.54312057930150	6.94949223618229	9.62949965626905
C	2.32493295803008	4.64441712672253	9.43341734757618
H	2.97693934014233	4.69690294909214	10.30337200878787
H	2.93278791399817	4.37064186324769	8.56847004871956
H	1.60883162755928	3.83758208153017	9.60580462694626
C	-0.76384784701415	5.91459212525861	12.14336961002323
H	-1.51677870727080	5.24862135069622	12.54684475854062
C	1.66907987049212	8.68649574919055	14.42778201473890
H	0.99628136481407	8.11316267115885	15.07127291969394
H	2.04279892206141	9.54129965490548	14.99334713139407
H	2.51742154458322	8.04391261441224	14.18780332778318
C	-0.23430705073867	10.04408193903044	13.52672032652308
H	-0.77467437694076	10.40331712874217	12.64899207448055
H	0.13480186593984	10.91130590971899	14.07886368806167

H	-0.94936482018002	9.52340498360228	14.16855296993084
C	10.21690093963371	8.19530502114560	12.06456846798215
H	10.22622894427748	7.12782005112715	12.34786040698673
H	9.72504801004832	8.73775084703908	12.87466043060405
C	11.64254780849936	8.69104172707876	11.78085795885597
H	11.79064528269803	9.70354637142304	12.15589785901889
H	12.37975590542763	8.05747598899090	12.27220181886025
C	0.68097089694762	5.81341702232396	7.96913498152792
H	-0.10734249588841	5.08457245608018	8.17031379457089
H	1.25173803211122	5.44794532703592	7.11179320998480
H	0.19674261718390	6.74989343218663	7.68435297781492
C	11.77198187103940	8.64528508744403	10.24203752868448
H	11.89770958149841	9.64996199603642	9.83805253041270
H	12.62682971729038	8.05626010910616	9.91233487816985
H	0.05173998417086	10.30415687520781	8.55588994402277
H	-0.34902109496009	9.79183954728690	10.19693116363884
H	-0.20937260574232	8.59815181143096	8.91993751726999

Optimized geometry of $[Fe(^{Pyrr}PDI)(NO)_2]^+$ (**5**) at the BP86/def2-TZVP(-f) level

Energy at this geometry = -2795.026396870172 Hartree

Fe	6.590011	5.504980	2.752956
O	5.121920	7.565976	1.520325
O	8.714020	5.700368	0.931989
N	5.604947	3.510897	2.142853
N	6.029567	4.575139	4.478659
N	7.408402	6.727003	4.255024
N	10.546455	8.640188	3.501641
N	5.554429	6.631681	2.070648
N	7.944966	5.382543	1.754605
C	4.316169	1.566059	3.006406
H	4.771158	0.775947	3.621855
H	3.286578	1.707010	3.370385
H	4.277315	1.227245	1.966078
C	5.088986	2.846053	3.125527
C	5.316321	3.427702	4.471496
C	4.861258	2.855498	5.665221
H	4.285604	1.931693	5.647202
C	5.160506	3.482216	6.876112
H	4.817938	3.052078	7.816980
C	5.905586	4.660523	6.871959
H	6.156398	5.159692	7.806356
C	6.329742	5.189510	5.646378
C	7.122069	6.424604	5.487423
C	7.499786	7.211872	6.707985
H	8.146517	6.612743	7.366851
H	8.031190	8.135227	6.464509
H	6.600251	7.474323	7.285879
C	8.229911	7.887387	3.908962
H	7.972292	8.752789	4.538237
H	8.018902	8.161612	2.868833
C	9.740113	7.563651	4.026965
H	9.979684	7.329617	5.090773
H	9.946014	6.653324	3.444480

C	10.646298	9.829780	4.363329
H	10.869351	9.534409	5.414266
H	9.702798	10.394785	4.367542
C	11.818641	10.636247	3.768000
H	12.427721	11.082125	4.564398
H	11.452398	11.457507	3.139547
C	12.619375	9.606266	2.920354
H	13.686153	9.586418	3.176943
H	12.538931	9.845018	1.851697
C	11.941057	8.262240	3.212408
H	11.979102	7.559772	2.367340
H	12.412463	7.769443	4.091408
C	5.513515	3.044703	0.786817
C	4.396692	3.402477	-0.006983
C	4.369239	2.945410	-1.331610
H	3.515868	3.198978	-1.962318
C	5.402201	2.175925	-1.859494
H	5.354550	1.829105	-2.892148
C	6.500670	1.855831	-1.064635
H	7.310083	1.258583	-1.486546
C	6.591037	2.283639	0.265544
C	3.235774	4.242660	0.517298
H	3.501381	4.599474	1.524514
C	2.983509	5.482384	-0.360867
H	2.208344	6.117718	0.091710
H	3.892361	6.085890	-0.485679
H	2.631896	5.200257	-1.363170
C	1.946383	3.405712	0.641639
H	1.130832	4.012855	1.060912
H	1.619951	3.041340	-0.342915
H	2.085372	2.528113	1.287766
C	7.798326	1.887205	1.110814
H	7.806869	2.528112	2.006030
C	7.693091	0.422310	1.582361
H	8.547250	0.160743	2.224649
H	6.771708	0.234607	2.151241
H	7.695640	-0.263247	0.722338
C	9.134225	2.106928	0.377309
H	9.974491	1.935458	1.065793
H	9.256834	1.405569	-0.460108
H	9.220683	3.126048	-0.021717

BS(0,0) optimized geometry of [Fe(^{Pyrr}PDI)(NO)]$^{+}$ (**9**) at the ωB97X-D3/def2-TZVP(-f) level

```
Energy of BS(0,0) at this geometry = -2664.408919 Hartree
Energy of BS(2,2) at this geometry = -2664.415207 Hartree
  Fe  9.07161662921278      5.11177931708051     10.21101634352971
  O   10.01900968631902      6.90318436975548      8.48036993289948
  N   7.24935992115287      5.91333066329239     10.66847949000975
  N   8.06790398702888      4.64248671899571      8.72757260888879
  N   9.99807150016234      3.52720236766263      9.64844849865235
  N   10.13895125805085      4.76129376501213     12.04315145570991
  N   9.84694649197767      6.36830688453722      9.50041743712405
  C   5.22936120870004      6.86774146098841      9.59389058946922
```

H	4.40563040914980	6.32176715325307	9.13473345333154
H	4.92803298574213	7.19823233045982	10.58488729873815
H	5.43006566872733	7.74891475042223	8.97863497605177
C	6.46327250444221	6.03473021934862	9.65051323769305
C	6.88131704857051	5.23274626767732	8.50086006123474
C	6.15834750121236	4.93402059648260	7.36142394273590
H	5.20409508020542	5.40650602238647	7.17345044230718
C	6.65992291531541	3.98623650444628	6.47620804708264
H	6.09761095464337	3.71935367406209	5.59167306616851
C	7.86090240723133	3.35271175167304	6.74718476945354
H	8.24202878793334	2.59034489780278	6.08230712394889
C	8.55051354620669	3.69144423184319	7.90248323682547
C	9.72123203992745	3.04741825989769	8.47872993069550
C	10.40271549897244	1.90362306529169	7.80409625093448
H	10.41316552319707	2.05536782851009	6.72473698254518
H	11.43222317975648	1.78710097885365	8.13675062761917
H	9.86991395124952	0.97354559069555	8.01560378399138
C	10.97544219456155	2.97156123124549	10.56162732653900
H	11.86445038900908	2.59085369017272	10.05378902592270
H	10.50066949156763	2.13081877475408	11.07659455536621
C	11.35579502190735	4.06846580573115	11.54506506043363
H	11.95691445191458	3.65600237506993	12.35974816641139
H	11.95811678486230	4.81483545826289	11.02493797682386
C	9.42239192695844	3.94740307974222	13.05755875656501
H	9.27260992157922	2.92794366096169	12.70296354227279
H	8.44346949617946	4.40597322978661	13.19522181351625
C	10.23548531900517	4.06716093974711	14.34832436606406
H	11.01348570227545	3.30398024134190	14.40233524624831
H	9.59563983964646	3.93113730044211	15.21932312976218
C	10.85356640352596	5.47994750541400	14.26129742174735
H	10.41771444429145	6.15527405940724	14.99483466934525
H	11.92856020161260	5.46614771905533	14.44309455110809
C	10.51338719686107	5.96108852976525	12.83806709512086
H	9.63764715862472	6.60578044438032	12.86631863511185
H	11.31716774938675	6.49974417557143	12.33769990970390
C	6.88165572623142	6.41614054190649	11.95834209278382
C	6.17841868582708	5.53651041604944	12.79931347457065
C	5.90437078609335	5.96012594801252	14.09177927407941
H	5.35258664076829	5.31197773322270	14.76129181518700
C	6.32403541235646	7.20200805814650	14.53942530501314
H	6.09155921991499	7.51970456844659	15.54888824428319
C	7.00158426593417	8.05213642419169	13.68573450041198
H	7.30062346324586	9.03096089768266	14.04224160967485
C	7.27985389489956	7.68968962647634	12.36950496003602
C	5.65743363007721	4.20499518560076	12.27991331528999
H	6.31761697666647	3.88633727326881	11.46835066566931
C	4.24307490234158	4.38317521174440	11.71361700046425
H	3.86257665647900	3.43918079913312	11.31667597405247
H	3.56747371333805	4.73029619184957	12.49912264433691
H	4.20361997439802	5.11474363564717	10.91356822148841
C	5.64012081717011	3.08174114970336	13.31401374432152
H	5.32844778313387	2.15410279207935	12.82879813970458
H	6.61909963320758	2.91941740021814	13.77015866086225
H	4.92991345610340	3.27722534354110	14.11885215943251
C	7.87645572955345	8.70073142620353	11.40169065548685

H	7.94024400061515	8.22396357392896	10.42283079793977
C	6.93574868042874	9.90074218773356	11.26180149736751
H	7.30334539477478	10.58595965542907	10.49683423886073
H	5.92926133061798	9.58100174368722	10.98192090891218
H	6.86297785548188	10.45931427375001	12.19691435826319
C	9.28997270035076	9.16303587485753	11.76890221147442
H	9.58214720435251	9.99856367558601	11.13233889957875
H	9.35902781517867	9.50066851139292	12.80558434856911
H	10.02072927160295	8.37078198922829	11.61389544618207

BS(2,2) optimized geometry of [Fe(^{Pyrr}PDI)(NO)]$^{+}$ (**9**) at the ωB97X-D3/def2-TZVP(-f) level

```
Energy of BS(0,0) at this geometry = -2664.398715 Hartree
Energy of BS(2,2) at this geometry = -2664.421295 Hartree
```

Fe	9.06983201666761	5.07740435666654	10.21613550942069
N	7.21737679050455	5.87071942943680	10.69159762138608
N	8.07194881887822	4.59715800793347	8.73576394436053
N	10.04362361783781	3.54407673399051	9.61480907942667
C	5.13961810899085	6.70423372527075	9.61411828674436
H	4.31920027066275	6.07256051808646	9.27556889967659
H	4.88127794376463	7.13564567199568	10.57767634338949
H	5.25468139214166	7.51395807640266	8.88915691479450
C	6.41207082066876	5.92788198002013	9.67979271658704
C	6.84353644190195	5.13161498014856	8.53665074999220
C	6.11870734726884	4.81169866438731	7.41397246903872
H	5.13537236955337	5.23273593044687	7.25453899713099
C	6.65467782895570	3.90391960621836	6.49224785389089
H	6.08420408770105	3.62145206592739	5.61822691906455
C	7.89433800941111	3.34125704960815	6.72014138234263
H	8.30081658542041	2.61842981398005	6.02651032250673
C	8.59812540228392	3.68474131732226	7.87208808896734
C	9.80089840410789	3.11044966457561	8.40355158438530
C	10.68627822322528	2.17094270348980	7.65353363136677
H	10.14884256448797	1.66182379425883	6.85629525484762
H	11.50249310405887	2.73706776250760	7.19581263010059
H	11.12571898418407	1.41522350514188	8.30264542095272
O	10.18267242405641	7.28074754949536	8.80861945056573
N	9.90010130992831	6.51088196421721	9.64037269280484
N	10.10073680184401	4.68547671609180	12.01797644360294
C	11.07947389319554	3.01678753493979	10.47688101525966
H	11.99515112973848	2.76261926416329	9.93894696364108
H	10.69988679105688	2.09908547994987	10.93752101178845
C	11.36825235015479	4.07758985508058	11.52662570170175
H	11.95909568209538	3.65828246224809	12.34428499576451
H	11.94459609585143	4.88234871575686	11.06851737135808
C	9.38786834566338	3.77793621986303	12.95350375025700
H	9.30331077546781	2.77883552262350	12.52835604050331
H	8.38407495750394	4.18458055715613	13.08269891650006
C	10.15640274596709	3.84886945257155	14.27401204470358
H	10.95968918565705	3.11139978943291	14.30585155603010
H	9.49851496600565	3.63505604502966	15.11513473134762
C	10.72209149265040	5.28593129699557	14.29457968666568
H	10.24159839233479	5.89685148175673	15.05556444114069
H	11.79130831274039	5.29737399123416	14.50679360528122

C	10.40850728783818	5.84553778590717	12.89407324090328
H	9.51650431437537	6.46694840216846	12.93013924822859
H	11.21476830280292	6.42848284462827	12.45101058547712
C	6.85885284611104	6.43088148303815	11.96365373554784
C	6.09567122331545	5.62901394407220	12.82898175741967
C	5.82572396500004	6.12252957717883	14.09854551074659
H	5.22812125215764	5.53295124622234	14.78308311003952
C	6.30097435579606	7.35704256629454	14.50256390654297
H	6.06763073697975	7.72842174290256	15.49334974175274
C	7.03884854000103	8.13272725604102	13.62825382773443
H	7.38339297094072	9.10876820819072	13.94903548869286
C	7.31774570836291	7.70003578846434	12.33435914493768
C	5.49446026659896	4.30617210767049	12.38087705576260
H	6.06407633560409	3.95258098818173	11.51825719852124
C	4.03553624771797	4.51598602534443	11.95375616819651
H	3.60337026393362	3.58648226349484	11.57671112068357
H	3.44293096508922	4.85924840511044	12.80566101833331
H	3.93208271557689	5.26734985419379	11.17878727737714
C	5.55453311991756	3.20856433971246	13.44160046860549
H	5.19329828210483	2.27069982467520	13.01476568354116
H	6.56783521251676	3.04518746645745	13.81396566114664
H	4.92111020257076	3.44058673641844	14.29896537886662
C	7.98379370711916	8.64308653409671	11.34570573999657
H	8.08346793930330	8.11358784648921	10.39874479968798
C	7.08163823628293	9.85355053080235	11.09358451253653
H	7.52402951859552	10.50499186835148	10.33843761849177
H	6.09545631123436	9.54144309006296	10.74264689469052
H	6.94408619487897	10.44322643075946	12.00189923782435
C	9.38556021635914	9.09457581132065	11.76098190985099
H	9.77299845209794	9.81045836057601	11.03539670873633
H	9.39075118558109	9.58220972230014	12.73811304757052
H	10.08247833864681	8.25976169245135	11.79574816226755

BS(0,0) optimized geometry of [Fe(^{Pyrr}PDI)(NO)]$^{+}$ (**9**) at the PBE0/def2-TZVP(-f) level

Energy of BS(0,0) at this geometry = -2662.888975262288 Hartree

Fe	9.00888441110378	5.01982165990695	10.26143165296807
N	7.18511289892506	5.85338609929824	10.72924060180011
N	8.02979944372898	4.59192906747587	8.76458958075843
N	10.02423928701653	3.55411592558544	9.60972209404410
C	5.15778302018106	6.77034646146563	9.63370568186087
H	4.33364631730637	6.20871973771221	9.19145043430875
H	4.86109228508466	7.12468395533188	10.61824517347576
H	5.34078188491796	7.64016259118439	8.99484238482172
C	6.39395337541189	5.94537441642464	9.69908035187734
C	6.82663777240534	5.17191614280757	8.55073710120649
C	6.14361832565304	4.94060345351041	7.37490142923835
H	5.18192714100381	5.40306867450296	7.19719406672796
C	6.69998538349707	4.08128150845834	6.42433637302488
H	6.16794142959913	3.87632998250207	5.50451648846995
C	7.91727590769149	3.46977841317357	6.67003166033657
H	8.34154149864121	2.78621884503036	5.94633064233753
C	8.57833356778778	3.72495461082748	7.86743476976662

C	9.77840677063726	3.14192512115914	8.38647906579917
C	10.66417443800532	2.21569236586458	7.63363086777737
H	10.16680800977857	1.80948433166873	6.75515974946006
H	11.55911786162573	2.74735088506570	7.29279823650965
H	10.99497756086556	1.37927810019498	8.25202304831219
O	10.23531537200272	7.01632822344449	8.72468802635845
N	9.86972588073365	6.41582230134468	9.65643297163627
N	10.04521605728589	4.58904696327496	12.03738630045863
C	11.11853891994386	3.06824134450015	10.41834349652917
H	12.03899152349252	2.93239817595912	9.84274839334531
H	10.85118444259976	2.08867318667606	10.83133777661933
C	11.34445863167369	4.08760539967668	11.51942949788359
H	11.95938934563396	3.66605333735657	12.32033581451108
H	11.87120833636886	4.94898037598574	11.10518165468275
C	9.39962643405116	3.57147093377299	12.90579317081647
H	9.41433849059660	2.59330179244295	12.42555820991135
H	8.35975653257351	3.87119122889967	13.03363359832449
C	10.13830150755549	3.62718702885805	14.24219058431341
H	10.97712751204274	2.92916095700938	14.26059447625812
H	9.47749454780307	3.34418928912595	15.06190741592305
C	10.62696708214358	5.08471815726803	14.34198608897397
H	10.13055579133236	5.62614554694824	15.14603056293465
H	11.69856804324992	5.13309269364226	14.54001306643524
C	10.27251178252640	5.70892449627500	12.98384303854477
H	9.34175316781588	6.27257142075027	13.05172651321232
H	11.04328636753521	6.36987891482870	12.58636501346720
C	6.83105764825947	6.46475850592838	11.97395091376516
C	6.13168803755273	5.67576702115972	12.90714136238450
C	5.84214934955481	6.24140309776749	14.14354866665138
H	5.29912492411850	5.66246902272074	14.88041703358118
C	6.22522209239952	7.53607937291927	14.44956033598468
H	5.98148067990383	7.95750222638320	15.41782386644265
C	6.90083566757071	8.29507309302810	13.51369675860752
H	7.18210224474623	9.31258604602637	13.75893270946215
C	7.21370851579657	7.78546299868895	12.25522296334469
C	5.63964560796648	4.27964535989978	12.56725994305442
H	6.30370747453131	3.87135948807274	11.79736550655110
C	4.22412763125776	4.32873950520170	11.98577130520766
H	3.87928255988830	3.32331755516148	11.73299544354544
H	3.53079929550958	4.75205656350201	12.71755287376321
H	4.16137938326318	4.93842986813196	11.08691644339324
C	5.65108093794291	3.31965614920830	13.75168876922949
H	5.38994135901177	2.31596523214154	13.40806929254349
H	6.62455012022862	3.27260506220228	14.24343172966375
H	4.91340283084927	3.59842754545746	14.50646758475402
C	7.89961587444529	8.67807663912264	11.24035428382642
H	7.98948799197446	8.11756130005527	10.30784817066390
C	7.07111184525397	9.92858105432074	10.95252621475562
H	7.55395420440622	10.52663377438210	10.17626414501429
H	6.06282771992310	9.67916703171633	10.61499819755271
H	6.98087746536059	10.55772591636383	11.84095227620677
C	9.31116390493635	9.07735260339334	11.66848966381009
H	9.77786200032868	9.68883194906072	10.89316691558204
H	9.30025710957087	9.66484324560817	12.59037479184349
H	9.94590116362038	8.20725865518433	11.83253471279323

BS(2,2) optimized geometry of [Fe(^{Pyr}PDI)(NO)]$^{+}$ (**9**) at the PBE0/def2-TZVP(-f) level

```
Energy of BS(0,0) at this geometry = -2662.8729076156  Hartree
Energy of BS(2,2) at this geometry = -2662.8890048088  Hartree
  Fe      9.008239      5.019013     10.261241
  N       7.183988      5.852642     10.728981
  N       8.030134      4.593054      8.763696
  N      10.024610      3.553984      9.607673
  C       5.155705      6.768283      9.633780
  H       4.332184      6.205845      9.191575
  H       4.858662      7.122226     10.618376
  H       5.337994      7.638273      8.994978
  C       6.393141      5.944933      9.698572
  C       6.826665      5.172499      8.550066
  C       6.143481      4.941758      7.374156
  H       5.181311      5.403586      7.197430
  C       6.700212      4.083508      6.422869
  H       6.168180      3.879181      5.502884
  C       7.917593      3.472286      6.668375
  H       8.342263      2.789080      5.944481
  C       8.578837      3.726734      7.865860
  C       9.779016      3.143172      8.384046
  C      10.664066      2.217817      7.628748
  H      10.157693      1.795310      6.763098
  H      11.547369      2.755496      7.267556
  H      11.013610      1.392942      8.252023
  O      10.253701      7.014353      8.737507
  N       9.875185      6.413001      9.663457
  N      10.043120      4.585793     12.037820
  C      11.118590      3.068226     10.416856
  H      12.039999      2.934050      9.842432
  H      10.851177      2.088197     10.828731
  C      11.342973      4.086707     11.519139
  H      11.958537      3.664824     12.319452
  H      11.868699      4.949037     11.105697
  C       9.400916      3.567338     12.907468
  H       9.418630      2.588662     12.428312
  H       8.360021      3.863774     13.034913
  C      10.139245      3.626698     14.243870
  H      10.979931      2.930967     14.263485
  H       9.478732      3.343008     15.063574
  C      10.624693      5.085390     14.341931
  H      10.127361      5.626876     15.145324
  H      11.696227      5.135853     14.539767
  C      10.269035      5.707231     12.983045
  H       9.337690      6.269938     13.050601
  H      11.039017      6.368463     12.584629
  C       6.830492      6.464782     11.973401
  C       6.131490      5.676307     12.907478
  C       5.841603      6.242708     14.143399
  H       5.298735      5.664221     14.880773
  C       6.224136      7.537758     14.448580
  H       5.979985      7.959750     15.416520
  C       6.899746      8.296025     13.512236
```

H	7.181186	9.313649	13.756912
C	7.212707	7.785804	12.254003
C	5.640512	4.279410	12.569334
H	6.305281	3.870540	11.800356
C	4.225117	4.326603	11.987387
H	3.879912	3.320752	11.736985
H	3.531971	4.751868	12.718239
H	4.162542	4.934211	11.087115
C	5.651657	3.321306	13.755288
H	5.393515	2.316666	13.412128
H	6.624151	3.276069	14.249212
H	4.912041	3.599827	14.508222
C	7.899047	8.678162	11.239461
H	7.989367	8.117933	10.306782
C	7.071577	9.929581	10.951912
H	7.555553	10.527738	10.176469
H	6.063137	9.681714	10.613788
H	6.981971	10.557830	11.841015
C	9.310678	9.077197	11.668077
H	9.778708	9.685784	10.891372
H	9.299137	9.667537	12.588187
H	9.944317	8.207001	11.835625

*Crystallographic Data for **3***: $C_{29}H_{38}FeN_4O_2$, M = 530.48, 0.4 × 0.31 × 0.2 mm, T = 100(2) K, Monoclinic, space group $P2_1/n$, a = 12.7147(5) Å, b = 13.7514(5) Å, c = 16.3476(7) Å, β = 108.215(4) °, V = 2715.1(2) Å^3, Z = 4, Dc = 1.298 Mg/m^3, μ= 0.588 mm^{-1}, F(000) = 1128.0, $2\vartheta_{max}$ = 54.204°, 23324 reflections, 5963 independent reflections [R_{int} = 0.0393], R1 = 0.0426, wR2 = 0.0946 and GOF = 1.055 for 5963 reflections (344 parameters) with I>2σ(I), R_1 = 0.0336, wR_2 = 0.0865 and GOF = 1.055 for all reflections, max/min residual electron density + 0.41/-0.38 eÅ^{-3}.

Crystallographic Data for **4**: $C_{29}H_{38}FeN_4O_3$, M = 546.48, 0.23 x 0.17 x 0.08 mm, T = 150(2) K, Monoclinic, space group $P2_1/c$, a = 16.165(2) Å, b = 9.9467(14) Å, c = 17.475(3) Å, β = 95.499(2)°, V = 2796.8(7) Å^3, Z = 4, D_c = 1.298 Mg/m^3, μ(Mo) = 0.575 mm^{-1}, F(000) = 1160, $2\vartheta_{max}$ = 50.48°, 56758 reflections, 6744 independent reflections [R_{int} = 0.0289], R1 = 0.0354, wR2 = 0.0914 and GOF = 1.040 for 6744 reflections (486 parameters) with I>2σ(I), R1 = 0.0418, wR2 = 0.0977 and GOF = 1.040 for all reflections, max/min residual electron density +0.421/-0.288 eÅ^{-3}.

Crystallographic Data for **5**: $C_{51}H_{58}BFeN_6O_2$, M = 853.69, 0.16 x 0.14 x 0.13 mm, T = 173(2) K, Triclinic, space group P-1, a = 10.4011(7) Å, b = 14.4990(17) Å, c = 15.8935(18) Å, α = 77.913(6)°, β = 75.424(6)°, γ = 84.359(6)°, V = 2265.6(5) Å^3, Z = 2, D_c = 1.251 Mg/m^3, μ(Cu) = 3.029 mm^{-1}, F(000) = 906, $2\vartheta_{max}$ = 133.39°, 27378 reflections, 7963 independent reflections [R_{int} = 0.0582], R1 = 0.0409, wR2 = 0.1110 and GOF = 1.094 for 7963 reflections (550 parameters) with I>2σ(I), R1 = 0.0588, wR2 = 0.1149 and GOF = 1.094 for all reflections, max/min residual electron density +0.439/-0.472 eÅ^{-3}.

Crystallographic Data for **6**: $C_{55}H_{66}BFeN_6O_4$, M = 941.79, 0.16 x 0.12 x 0.09 mm, T = 173(2) K, Triclinic, space group P-1, a = 10.5114(3) Å, b = 15.2880(4) Å, c = 17.6141(5) Å, α = 71.067(2)°, β = 76.115(2)°, γ = 72.057(1)°, V = 2516.18(13) Å^3, Z = 2, D_c = 1.243 Mg/m^3, μ(Cu) = 2.805 mm^{-1}, F(000) = 1002, $2\vartheta_{max}$ = 133.28°, 27889 reflections, 8852 independent reflections [R_{int} = 0.0481], R1 = 0.0543, wR2 = 0.1567 and GOF = 1.079 for 8852 reflections (604 parameters) with I>2σ(I), R1 = 0.0600, wR2 = 0.1616 and GOF = 1.079 for all reflections, max/min residual electron density +0.775/-0.600 eÅ^{-3}.

Crystallographic Data for **9**: $C_{51}H_{58}BFeN_5O$, M = 823.68, 0.17 x 0.16 x 0.11 mm, T = 173(2) K, Triclinic, space group P-1, a = 11.3063(4) Å, b = 14.0433(5) Å, c = 14.6725(5) Å, α = 81.601(2)°, β = 85.289(2)°, γ = 71.560(2)°, V = 2184.75(14) Å^3, Z = 2, D_c = 1.252 Mg/m^3, μ(Cu) = 3.097 mm^{-1}, F(000) = 876, $2\vartheta_{max}$ = 133.23°, 26251 reflections, 7692 independent reflections [R_{int} = 0.0424], R1 = 0.0355, wR2 = 0.0963 and GOF = 1.048 for 7692 reflections (532 parameters) with I>2σ(I), R1 = 0.0379, wR2 = 0.0976 and GOF = 1.048 for all reflections, max/min residual electron density +0.569/-0.478 eÅ^{-3}.

*Crystallographic Data for **10***: $C_{51}H_{58}BFeN_5O_2$, M = 839.68, 0.29 × 0.27 × 0.20 mm, T = 100(2) K, Triclinic, space group P-1, a = 9.14310(10) Å, b = 12.8888(2) Å, c = 19.5058(3) Å α = 91.1090(10)°, β = 97.2010(10)°, γ = 101.1230(10)°, V = 2235.43(6) Å^3, Z = 2, Dc = 1.247 Mg/m^3, μ= 0.383 mm^{-1}, F(000) = 892.0, $2\vartheta_{max}$ = 52.744°, 34528 reflections, 9128 independent reflections [R_{int} = 0.0219], R_1 = 0.0318, wR_2 = 0.0759 and GOF = 1.045 for 9128 reflections (773 parameters) with I>2σ(I), R_1 = 0.0284, wR_2 = 0.0739 and GOF = 1.045 for all reflections, max/min residual electron density +0.36/-0.33 eÅ^{-3}.